

**DOKUZ EYLÜL UNIVERSITY**  
**GRADUATE SCHOOL OF NATURAL AND APPLIED SCIENCES**

**EFFECTS OF THE LINK AND JOINT  
FLEXIBILITIES ON THE DYNAMIC  
CHARACTERISTICS OF ROBOT  
MANIPULATORS**

by  
**Arjan I. SADEQ**

**October, 2011**  
**İZMİR**

**EFFECTS OF THE LINK AND JOINT  
FLEXIBILITIES ON THE DYNAMIC  
CHARACTERISTICS OF ROBOT  
MANIPULATORS**

**A Thesis Submitted to the Mechatronic Engineering Department of Dokuz  
Eylül University in Partial Fulfillment of the Requirements for the Degree of  
Master in Mechatronic Engineering**

**by  
Arjan I. SADEQ**

**October, 2011  
İZMİR**

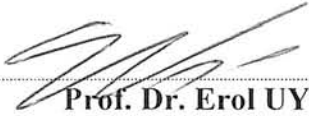
**M.Sc THESIS EXAMINATION RESULT FORM**

We have read the thesis entitled “EFFECTS OF THE LINK AND JOINT FLEXIBILITIES ON THE DYNAMIC CHARACTERISTICS OF ROBOT MANIPULATORS” completed by ARJAN I. SADEQ under supervision of ASSOC.PROF.DR. ZEKİ KIRAL and we certify that in our opinion it is fully adequate, in scope and in quality, as a thesis for the degree of Master of Science.



Assoc. Prof. Zeki KIRAL

Supervisor



Prof. Dr. Erol UYAR

(Jury Member)



Assist. Prof. Dr. Aysun BALTACI

(Jury Member)

**Prof. Dr. Mustafa SABUNCU**  
Director  
Graduate School of Natural and Applied Sciences

## **AKNOWLEDGMENTS**

During my graduate study I would like to thank the person who always show me the right way and expand my horizon by teaching me different view points Assoc. Prof. Dr. Zeki KIRAL, and during the lessons I would like to thank Prof. Dr. Erol UYAR who always trust and support me. Thank you to all my friends who supported me during my studies. And finally I would like to thank my family because without them I will never have done this.

Arjan I. SADEQ

# EFFECTS OF THE LINK AND JOINT FLEXIBILITIES ON THE DYNAMIC CHARACTERISTICS OF ROBOT MANIPULATORS

## ABSTRACT

Robots have a very significant position among the production tools in today's technology. The robots which execute the transactions such as mounting, painting, transportation, blanking, welding, section feeding, peening, supervision and drilling in the sectors such as automotive, machine production, textile, electronic, chemistry, food and medicine. Robots are preferred in industry and service sectors for the features such as sensitive production, being calculable, acquiring rapid and high quality products, existing in the conditions in which human cannot work and saving from the labor force, although their usage areas are different.

The selection and design of the serial and parallel manipulators are executed in accordance with the basic measures such as load capacity, precise positioning, iteration and rigidity in respect to the usage places and requirements. Computer-aided Engineering tools are utilized for fulfilling the requirements such as selection of the degrees of freedom and making the necessary geometric designation. In consequence of the computer based analyses and designs, the most effective manipulator selection is made and savings in respect of the costs is provided which is one of the most significant problems of the industry.

In this study, natural frequency analyses have been made by using the method of finite elements for the different positions of three independence grade serial manipulators in the study space. Then the finite elements analyses were repeated and the diversion of the natural frequencies were observed by changing the materials of the parts and rigidities of the junction pieces. The primary five natural frequency values for 190 different positions in the study space of the robot have been shown in three dimension graphics with the programme which was developed in MATLAB programme.

**Keywords:** 3-axes, robot serial manipulator, finite element theory, natural frequency, joint flexibility

# UZUV VE MAFSAL ESNEKLİKLERİNİN ROBOT MANİPÜLATÖRLERİNİN DİNAMİK KARAKTERİSTİKLERİ ÜZERİNE ETKİLERİ

## ÖZ

Günümüz teknolojisinde üretim araçları arasında robotun çok önemli bir yeri vardır. Otomotiv, makina-imalat, tekstil, elektronik, kimya, gıda ve tıp başta olmak üzere birçok sektörde montaj, boyama, taşıma, kesme, kaynak, parça besleme, yüzey işleme, denetleme ve delme gibi işlemleri gerçekleştiren robotlar yaygın olarak kullanılmaktadır. Kullanım yerleri farklı olmasına rağmen, robotlar hassas üretim yapabilme, güvenilir olma, seri ve kaliteli mamül elde etme, insanların çalışamayacağı koşullarda bulunabilme, iş gücünden tasarruf sağlama gibi özelliklerden dolayı sanayi ve hizmet sektöründe tercih edilmektedirler.

Yük kapasitesi, hassas konumlama, tekrarlama ve rijitlik gibi temel robot kriterlerine bağlı olarak, kullanım yeri ve ihtiyaçlara göre seri veya paralel manipülatörlerin seçimi ve tasarımı yapılmaktadır. Gerekli ihtiyaçları karşılamaya hizmet etmek amacıyla gerek serbestlik derecesinin seçimi, gerek uygun geometrik tasarımın yapılması için günümüz gelişen teknolojisinde Bilgisayar Destekli Mühendislik araçlarından yararlanılmaktadır. Bilgisayar tabanlı yapılan analiz ve tasarımlar sonucunda, en verimli manipülatör seçimi yapılmakta olup endüstrinin en büyük sorunlarından biri olan maliyet yönünden de tasarruf sağlanmış olur.

Bu çalışmada, deneysel amaçlı tasarlanmış üç serbestlik dereceli seri manipülatörün çalışma uzayı içerisindeki farklı konumları için sonlu elemanlar yöntemi kullanılarak doğal frekans analizleri yapılmış ve sonrasında bağlantı elemanlarının ve uzuvların malzemeleri değiştirilerek tekrar sonlu elemanlar yöntemi ile doğal frekans analizi yapılarak sistemin esnekliği incelenmiştir. Çalışma uzayı içerisinde 190 farklı konum için sistemin ilk beş doğal frekans değeri işlenerek MATLAB programında geliştirilen algoritma ile sonuçlar çalışma uzayı içerisinde üç boyutlu grafikte gösterilmiştir.

**Anahtar Sözcükler:** 3-eksenli, robot seri manipülatör, sonlu element yönetimi, doğal frekanslar, mafsal esnekliği

## CONTENTS

	<b>Page</b>
MASTER THESIS EXAMINATION RESULT FORM .....	ii
ACKNOWLEDGEMENTS .....	iii
ABSTRACT .....	iv
ÖZ .....	v
<b>CHAPTER ONE-INTRODUCTION .....</b>	<b>1</b>
1.1 Introduction .....	1
1.2 The Historical Development of the Industrial Robots.....	2
1.3 Literature Review .....	7
1.4 Objective of the Project .....	11
<b>CHAPTER TWO-ANALYSIS METHODS .....</b>	<b>12</b>
2.1 Analysis Methods in Robot Design.....	12
2.2 Operating envelope.....	12
2.2.1 Natural Frequency Concept .....	15
2.2.2 Natural Frequency Expression for an Embedded Beam: Lumped Parameter System Assumption .....	18
2.2.3 Natural Frequency Expression for an Embedded Beam: Distributed Parameter System Assumption .....	19
2.2.4 Different Studies on the Flexible Rotor Beam Element for the Manipulators with Joint and Link Flexibility .....	25
2.2.5 Flexible Rotor Beam Element Model .....	26
<b>CHAPTER THREE-TECHNICAL DATA OF THE ROBOT .....</b>	<b>29</b>
3.1 Technical Data of the Robot.....	29

3.2 Kinematic Analysis .....	32
3.3 Rigidity Analysis in Serial Manipulators .....	32
3.4 Rigidity Analysis in Serial Manipulators .....	32
<b>CHAPTER FOUR- THE NATURAL FREQUENCY ANALYSIS OF ALUMINUM .....</b>	<b>34</b>
4.1 The Natural Frequency Analysis of Aluminum .....	34
4.2 The Natural Frequency Analysis of the Steel.....	40
4.3 Examine The Effect of The Equivalent Arc Parameters to the Flexibility of the System By Utilizing From The Pin Connector Feature of the Solidworks Program .....	47
4.3.1 Torsion Spring Coefficient Quantization for the Aluminum.....	47
4.3.2 Torsion Spring Coefficient Quantization For The Steel.....	53
<b>CHAPTER FIVE- CONCLUSIONS AND SUGGESTIONS.....</b>	<b>59</b>
<b>REFERENCES .....</b>	<b>61</b>

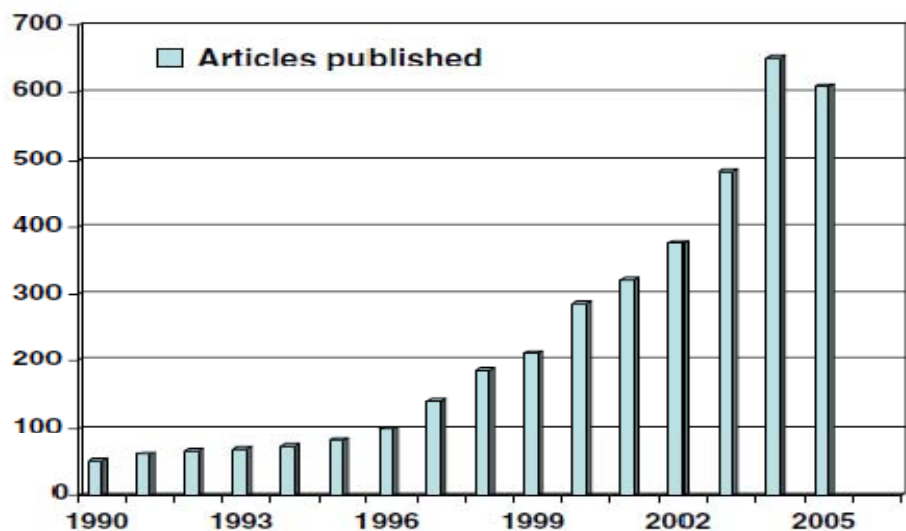


# CHAPTER ONE

## INTRODUCTION

### 1.1 Introduction

Robots have become incorporated into daily life over the last half century: what was once only science fiction has now become a reality. Today, everyone living in the developed world benefits from the advances in robotics in everyday life. Healthcare industries have all incorporated robotics to help improve efficiency and precision. Robots help to build our machines, package our foods, and wash our cars. While robots are commonly employed in the healthcare laboratory setting, they have been more slowly integrated into clinical medicine. Over the last two decades, research in surgical robotics has been continually increasing with a geometric rise in the number of manuscripts published each year, as shown in Figure 1.1. Surgical robotics is an evolving field aiming to take advantage of the features of robotics that have made them so valuable in other industries.



Number of articles indexed each year in a pubmed search containing the words “robot” or robotic. (Akdağ, 2008)

Figure 1.1 Number of articles indexed each year in a pubmed search containing the words “robot” or robotic. (Akdağ, 2008)

## 1.2 The Historical Development of the Industrial Robots

The industrial robots are defined as ‘automatic controlled, programmable, three or more axes, multi-functional manipulator programmes’ according to the ISO (ISO 1994) standards. The general implementation areas of the robots which are welding, painting, mounting, lifting and removal, packaging transactions are fulfilled with high speed and sensitiveness.

George Devol made the first robot patent application in 1954. Unimation company made the first robot production in reliance with George Devol’s patent. These robots produced were called ‘programmable transfer machines’. The usage areas of the programmable transfer machines is transferring an object from one point to another.

The first industrial robot is seen in Figure 1.2. Then the Unimation Technologies were licensed by Kawasaki Heavy Industries and Guest-Nettelfolds and its production was made in Japan and England. The only competitor of the Unimation company was Cincinnati Milacron Inc. Of Ohio for a while. Then several robot companies entered the industrial robot market.

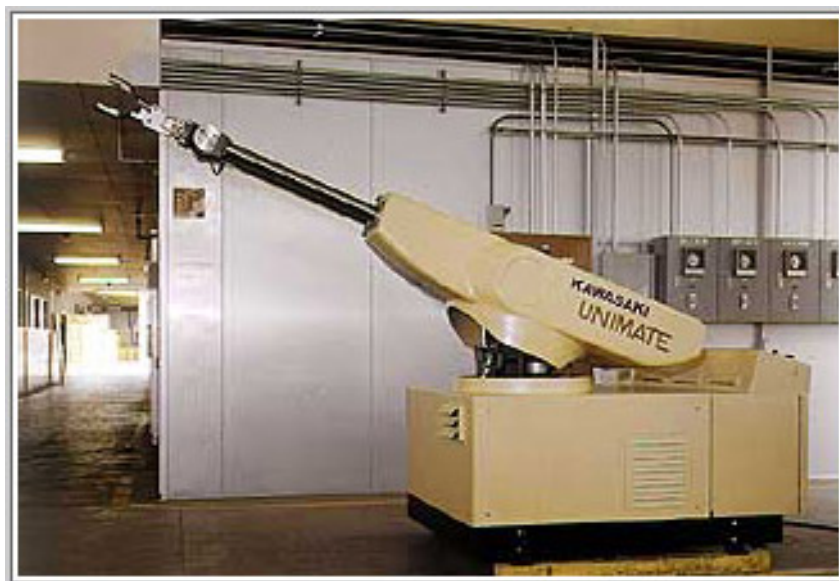


Figure 1.2 First industrial robot (Kawasaki Aircraft) (Akdağ, 2008)

In 1986 Marvin Minsky developed octopus like tentacle arms. Robot arm is seen in Figure 1.3.



Figure 1.3 Tentacle arm (Lynxmotion). (Akdağ, 2008)

In 1969, Victor Scheinman, who was a mechanical engineer in Stanford University developed Stanford Arm. The design of the Stanford Arm is still an impressive design in the present day. This is the first electrical and computer controlled robot which was developed in those years. Stanford manipulator, is shown in Figure 1.4.



Figure 1.4 Stanford manipulator (Victor Scheinman). (Akdağ, 2008)

In 1973, Cincinnati Milacron company introduced the first market-like mini-controlled industrial robots. This robot which was developed by Richard Hohn is shown in Figure 1.5.



Figure 1.5 Cincinnati Milacron company's first welding robot. (Akdağ, 2008)

In 1974 Victor Scheinman launched the Silver Arm by establishing his own company.

The feature of this robot is assembling of the little pieces by receiving feed-back from touching and pressure sensors. As shown in Figure 1.6.

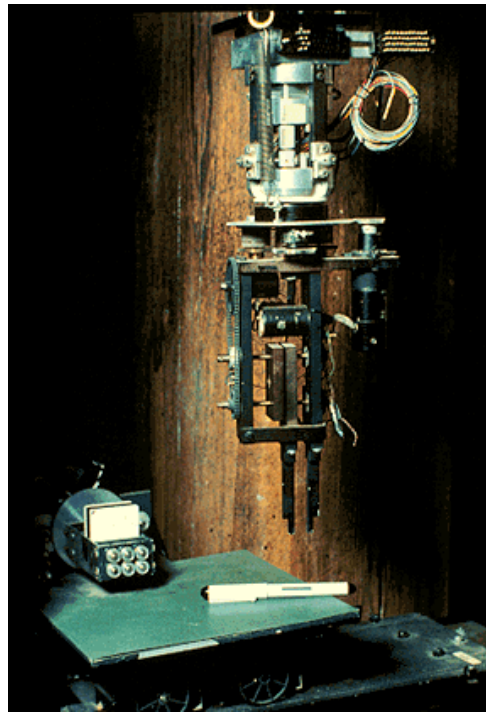


Figure 1.6 Victor Scheinman launched the Silver Arm (Scheinman Silver). (Akdağ, 2008)

Victor Scheinman developed the PUMA (Programmable Universal Manipulation Arm) which is used largely in the market. Unimation Company launched the PUMA robots in 1979 by using the technology that they received from Vicarm. The robot is shown in Figure 1.7.

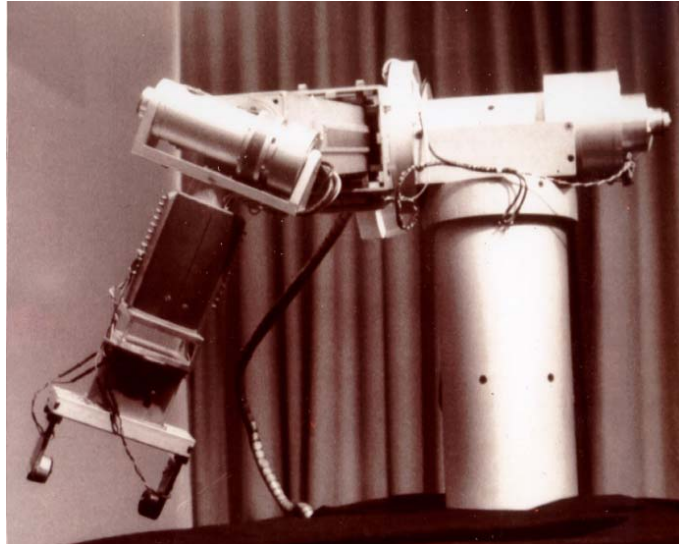


Figure 1.7 Vicot scheinman PUMA arm (Victor Scheinman, Hand-Eye Project, Stanford Artificial Intelligence Laboratory, 1969). (Akdağ, 2008)

Sankyo and IBM, introduced SCARA (Selective Compliant Articulated Robot Arm) by developing it in the Yamanashi University as shown in Figure 1.8.



Figure 1.8 Sankyo and IBM, introduced SCARA (Selective Compliant Articulated Robot Arm). (Akdağ, 2008)

In 1981, Takeo Kanade developed the direct drive arm. This robot is the first design in whose joints engine was settled.

In 1986, Honda began a robot research programme. The main theme of this programme is the movement of robots just like humans for the society to benefit.

In 1989, Rodney Brooks and A.M.Flynn published the 'Fast, Cheap and Out of Control: A Robot Invasion of the Solar System' article in British Interplanetary Society Magazine. This article argued that smaller, useful and cheaper robots should be developed instead of the big expensive ones.

In 2000, Honda introduced hominid ASIMO robot and this robot formed basis for the hominid robots. As shown in Figure 1.9.

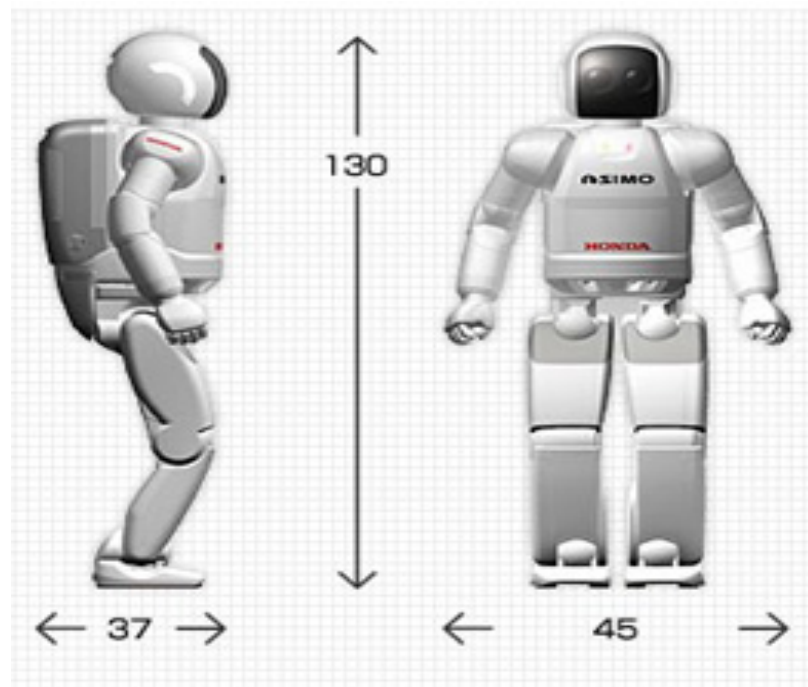


Figure 1.9 ASIMO the new generation of robot made by HONDA (The Honda Motor Company). (Akdağ, 2008)

In September 2000, 742.500 robots were in use all over the World and more than half of them were used in Japan.

In the recent years, the robot producers increased the researches of the light weight robots. In the Figure 1.10, the researches of Motoman's light weight robot, SDR10 and Kuka's light weight robot are seen.

In recent years robot producers are increasingly focusing on lightweight robot research. Figure 1.10 shows SDR10 lightweight robot of Motoman and lightweight robot research of Kuka.



Figure 1.10 Lightweight robots, applications of Motoman and Kuka (Motoman Robots). (Akdağ, 2008)

### 1.3 Literature Review

Today optimization of robot design is an important field of research. Increasing expectations in robot manipulator design has increased flexible production conditions. Being very complex structures, robot manipulators comprise various parameters and geometric planes. In optimum conditions Computer Assisted Engineering (CAE) methods are used for robot design.

The most important study setting the fundamentals of robotic design was conducted by Thomson (1984). Thomson has initially researched demands and requirements of designers and then applied his findings on practical field.

Vukobratovic, Potkonjak, Inoue and Takano (2002) have adapted robotic drive systems and CAD system for industrial robot design. Instead of providing final solutions, they have defined rules for advanced robot design in their study.

Mir-Nasiri (2004) has designed a new robotic arm with a parallel structure similar to the SCARA robot in respect of application fields and geometrics. This new design is more advantageous and functional compared to the SCARA robot. In addition, the studies have been aimed to solve various potential problems in design, modeling and application stages.

Mrozek (2003) have made two new ventures in interdisciplinary mechatronics. First of these is UML (Unified Modelling Language) modeling, and the second is physical modeling with MODELICA. UML provides an advantage by facilitating understanding of graphical diagrams and modification of these in mechatronic systems.

Clark and Lin (2007) have used CAD integration method for analysis and corroboration of robot design mechanisms. This system provides ease of use and saves time with flexible design in robot mechanism design.

Myung and Han (2001) have defined parametric modeling processes of machine parts, and application of these parametric modeling processes on robot manipulators.

Lucchetta, Bariani and Knight (2005) have developed design, production and product simplification methods based on the Theory of Inventive Problem Solving (also known as TRIZ or TIPS).

Bhatia, Thirunarayanan and Dave (1998) have developed a new system for SCARA robot design. The objective of this study is to shorten the robot design process and enable production of more specialized robots.



Morozov and Angeles (2007) have focused on Schönflies-Motion Generator (SGM). Schönflies motions, consisting of three separate displacements and one translational, provide an advantage with four degrees of freedom. According to SGM plan the design protocol consists of: (i) modeling and imaging, (ii) determination of most distinctive parameters and characteristics for specialized design, (iii) design of primary parts, (iv) defining parameters of rigid and flexible bodies using form analyses, and (v) preparation of detailed design and production drawings.

Kim and Park (2007) have prepared a new humanoid robot hardware. They have formed the external structures of the robot by using CAD/CAM/CAI and rapid prototyping systems. In this study 3D CAD programs and CAE systems are mainly used for modal simulation and kinematic analyses. In result, humanoid robot prototype Bonobo was produced.

O'Halloran, Wolf and Choset (2005) have introduced a low-budget two-wheeler robot platform. In this study drive transmission system and suspension system were improved and vibration characteristics were optimized.

Ouyang, Li and Zhang (2003) have defined a Real Time Controllable (RTC) mechanism with power stabilization and trace tracking. They have created a new approach to RTC mechanism, called Adjustable Kinematic Parameters (ACP) approach. This new approach is much a more functional and promising system in respect of servomotor reduction of joint forces and torque.

Dwivedy and Eberhard (2006) have conducted the most comprehensive study on flexible robot manipulators. Their articles are divided under three sections as modeling, control and experimental studies.

Sun and Mills (1999) have defined a new adaptable control method named Adaptable-Control (A-L). This theory is studied under two sections as singular mode and repeating mode.

Young and Pickin (2000) have used three modern serial manipulators to compare robot precisions. Each robot has been subjected to laser measurement system. Test measurements were conducted only in static condition.

Drouet, Dubowsky and Mavroidis (1998) have developed a model stabilizing errors in end effectors. This method has been applied on a high precision medical robot with six degrees of freedom. This method distinguishes geometric errors from flexibility errors in end effectors.

Xu, Tso and Wang (1998) have studied sensor based modeling and control of position errors originating from structure of flexible manipulators.

Zhang and Goldberg (2005) have developed a fast, cheap and easy-to-control calibration system for a wafer-handling robot. This system is based on stabilization and simple compensation algorithm.

Shirinzadeh, Teoh, Foong and Liu (1999) have conducted dynamic measurements on mobile end effectors with a laser interferometer based sensor technique. In this system sensors were used for guidance of end effectors of the robot.

Karagulle and Malgaca (2004) have studied trajectory flexibility effects on a two membered planar manipulator using computer assisted engineering tools.

Akdag (2008) have developed rigidity space concept for robot manipulators and derived rigidity spaces for various types of robot manipulators.

Akdag and Kiral (2007) have studies effects of trajectory effect on dynamic stress values of an ABB robot.

#### 1.4 Objective of the Thesis

Due to geometric limitations and structural complications robot design has become a challenging problem. An industrial robot is expected to work with high speed and precision, as well as having a large operating envelope. Therefore multiple parameters must be considered simultaneously. Robot design is a demanding task even for professional designers. Today using CAE process in robot design has become unavoidable.

In this study, natural frequency analyses have been made by using the method of finite elements for the different positions of a three DOF serial manipulator in its work space. Then the finite elements analyses were repeated and the diversion of the natural frequencies were observed by changing the materials of the parts and rigidities of the joints. The primary five natural frequency values for 190 different positions in the work space of the robot have been shown in three dimensional graphics with the programme which was developed in MATLAB.

The analyses have been made by using steel and aluminum materials and it has been observed that the steel material exhibits a more rigid pattern during the movement of the manipulator. Then, the equivalent arc parameters were calculated in accordance with the material features and geometry of these junction pieces by removing the joint parts pieces. The effect of the equivalent arc parameters to the flexibility of the system was examined by utilizing from the pin connector feature of the SolidWORKS programme. The acquired results were shown in three dimensional graphics in work space.

Although the analyses results indicates that the manipulator which was derived from steel material is more rigid in the study space, we cannot reach the conclusion that steel material is effective for each usage area. Whether the flexibility of the system remains in acceptable limits for each of two materials, there can be areas in which aluminum material is preferred for reducing the weight and cost. Besides in consequence of the numeric analyses, it has been observed that joint flexibility changes have significant effect on the natural frequencies of the robot manipulators.

## **CHAPTER TWO**

### **ANALYSIS METHODS**

#### **2.1 Analysis Methods in Robot Design**

In recent years machine manufacturers have stepped up production competition by adjusting their production according to customer specifications. Instead of creating a lot of different models, it became more important to make customer specific productions with a slight increase in costs and quality. Customer specific production needs to be fast and effective, which gives rise to the need for flexible design. Flexible design can be defined as fast and reliable methods meeting the required conditions. Flexible designs are made by integrated CAE analyses.

Steps of integrated design analysis are shown Figure 2.1. This process starts with definition of work and ends with production of the robot. This process is used by large scale manufacturers and methods, programs and processes are not disclosed into open literature. However, integrated design steps are defined in a way understandable to any manufacturer.

#### **2.2 Operating envelope**

Operating envelope of a manipulator can be defined as the volume accessible by the end effector. There are two different current definitions of operating envelope. Operating envelope can also be defined as the volume accessible by each end effector on at least one orientation. The volume accessible by the end effector on every possible orientation is called maximum operating envelope. In short, expanded operating envelope is a sub-group of accessible operating envelope group.

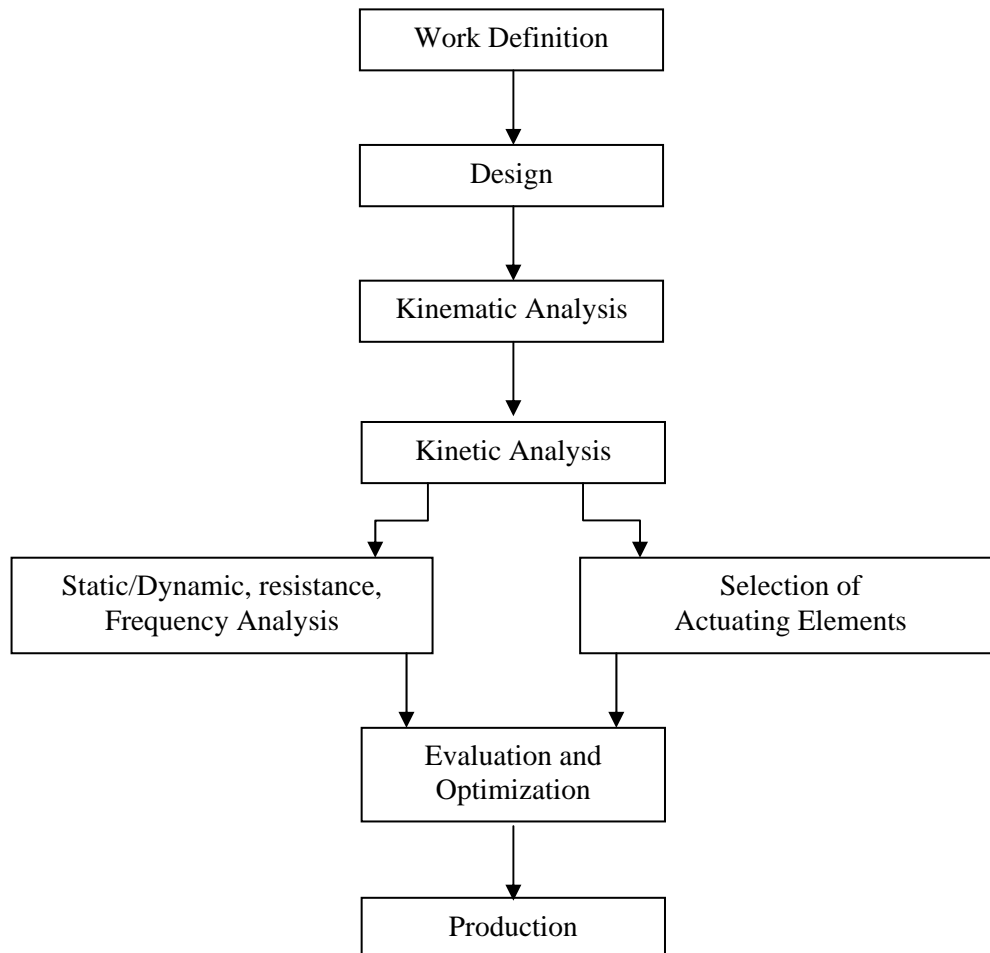


Figure 2.1 Steps of integrated design analysis (Akdağ, 2008)

Even though this is not a requirement, first three mobile members of most serial manipulators are designed longer than the other members. The first three members are used for positioning of end effector, while the other members are used for orientation. First three members are called the “arm”, while the other members are called the “wrist”. Except the manipulators with redundant axes, wrist components of manipulators have 1 to 3 degrees of freedom, while arms have three degrees of freedom in total. The axes conjoining at the wrist point forms the wrist hub. Formed by various kinetic elements, the arm covers wide operating envelopes to form operating envelope zone.

Presumably the most basic kinematic structure in robot arms consists of three sliding joints positioned at right angles to each other. These types of robots are known as Cartesian robots. Wrist hub point of a Cartesian robot can be defined as the

intersection point of three Cartesian coordinated with the three joints. Operating envelope zone of a Cartesian manipulator is a rectangular box. Figure 2.2 shows a Cartesian robot produced by Seiko Company



Figure 2.2 Cartesian robot produced by Seiko Company. (Akdağ, 2008)

If first or second joint of a Cartesian manipulator is replaced with a rotary joint, this robot is called a cylindrical robot. Wrist hub of the cylindrical robot can be defined as the intersection of cylindrical coordinates set and parameters of three joints. Generally mechanical limits of sliding joints are the two terminus points. Therefore operating envelope of cylindrical robots is limited to two concentric cylinders. A cylindrical robot is shown in Figure 2.3.



Figure 2.3 A cylindrical robot produced by Seiko Company. (Akdağ, 2008)

If the first two joints of the robot arm are rotary type and third joint is sliding type this type of robot is called a spherical robot. Normally the sliding joint is not parallel to second joint axis. Operating envelope of a spherical robot is limited by two concentric spheres. As shown in Figure 2.4 the Stanford manipulator which has a spherical operating envelope.



Figure 2.4 Stanford Manipulator. (Akdağ, 2008)

### ***2.2.1 Natural Frequency Concept***

Natural frequency of a mechanical system is a system-specific value defined as the free vibration frequency of the system (in absence of external stress). Number of natural frequencies is equal to number of degrees of freedom of the system. Since systems like beams have an unlimited number of degrees of freedom number of natural frequencies of such systems is also unlimited. However, since lumped parameter systems have a limited number of degrees of freedom, number of natural frequencies in these systems is equal to the number of degrees of freedom.

The model typically used to express natural frequency concept is the mass-spring system with single degree of freedom as shown in Figure 2.5.

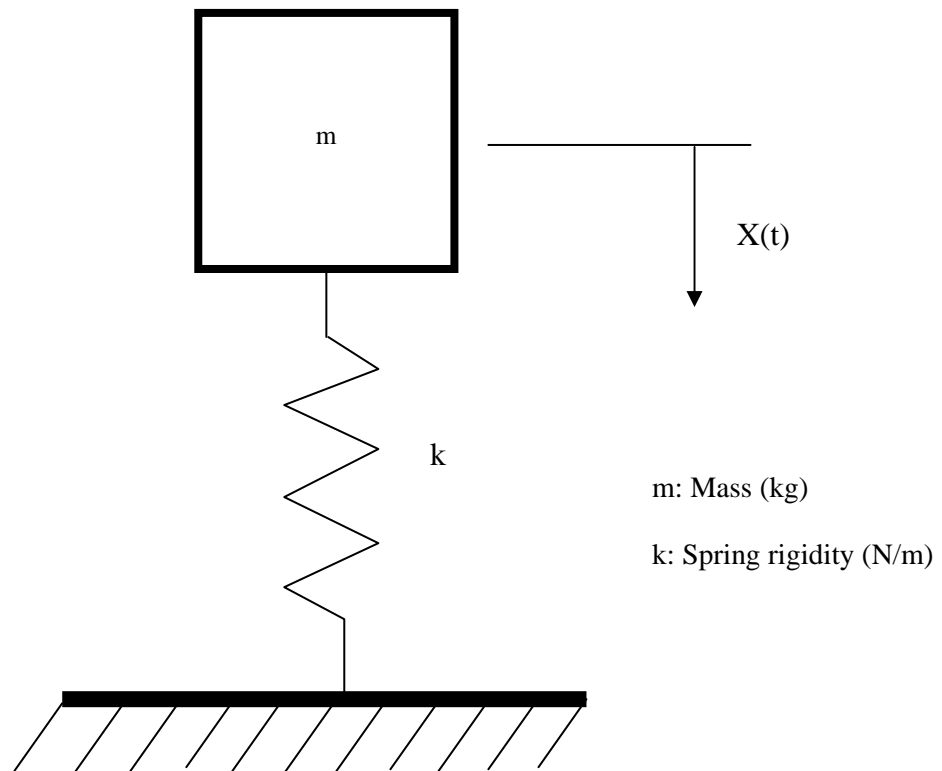


Figure 2.5 Mass-spring system with single degree of freedom

Displacement equation expressing the displacement of mass-spring system in absence of dampening and external stress  $x(t)$  can be shown as follows using Newton's 2nd Law or energy method and Lagrange's equation:

$$m\ddot{x} + kx = 0 \quad (2.1)$$

For the temporal  $x(t)$  displacement expression generated by an initial displacement effect applied on the mass is can be assumed;

$$x(t) = Ae^{st} \quad (2.2)$$

From here placing the  $x(t)$  and  $\ddot{x}(t)$  values in the equation:

$$\left[ m \quad s^2 + k \right] Ae^{st} = 0 \quad (2.3)$$



$$\left[ m \ s^2 + k \right] A = 0 \quad (2.4)$$

Keeping in mind that the coefficient A must take a value other than zero to derive a valid  $x(t)$  displacement, the  $s$  values giving  $m s^2 + k = 0$  expression will be values validating initially assumed  $x(t)$  solution. These values are defined as the natural frequency the mass-spring system with one degree of freedom and derived as follows;

$$s_{1,2} = \pm \sqrt{\frac{k}{m}} i \quad (\text{rad/sn}) \quad (2.5)$$

Here  $i = \sqrt{-1}$ . Since frequency concept in physical system will take a positive value, natural frequency a mass-spring system is found as;

$$\omega_n = \pm \sqrt{\frac{k}{m}} \quad (\text{rad./sn}), \quad f_n = \frac{1}{2\pi} \sqrt{\frac{k}{m}} \quad (\text{Hz}) \quad (2.6)$$

As seen in the natural frequency expression, natural frequency of a system is directly proportional with system rigidity and inversely proportional with system mass. Therefore, natural frequency of high rigidity systems will be higher compared to more flexible systems. The importance of natural frequency concept in robot design is related to natural vibration amplitudes observed during sudden starts and stops of robot manipulator. Systems with a high natural frequency will have a more rigid structure and in parallel their natural vibration amplitude will be smaller. This way, high amplitude vibration of robot manipulator in sudden starts and stops will be limited and manipulator precision will be increased. Robot manipulators typically do not have simple geometries which can be modeled as lumped parameter systems. However, natural frequencies of the robot manipulators do not allow manipulator structuring on a continuous system assumption either. These concepts are shown below for an embedded beam.

### ***2.2.2 Natural Frequency Expression for an Embedded Beam: Lumped Parameter System Assumption***

Natural frequency expression of the embedded beam shown on Figure 2.5 can be derived in a most simple way by assuming a system with a single degree of freedom formed by lumping the mass of beam on the desired point of the beam.

Using the equivalent model on the figure, natural frequency value of the embedded beam can be shown as :

$$\omega_n = \sqrt{\frac{k}{m}} = \sqrt{\frac{3EI}{L^3}} = \sqrt{\frac{3EI}{0.243 \times m_{beam} L^3}} = 3.514 \sqrt{\frac{EI}{m_{beam} L^3}} \text{ (rad/s)} \quad (2.7)$$

This natural frequency value is derived for the model with single degree of freedom on the assumption of whole beam mass being lumped on a single point on the free end of the beam. Since the embedded beam is simplified for examination in this model the derived natural frequency value is also approximate.

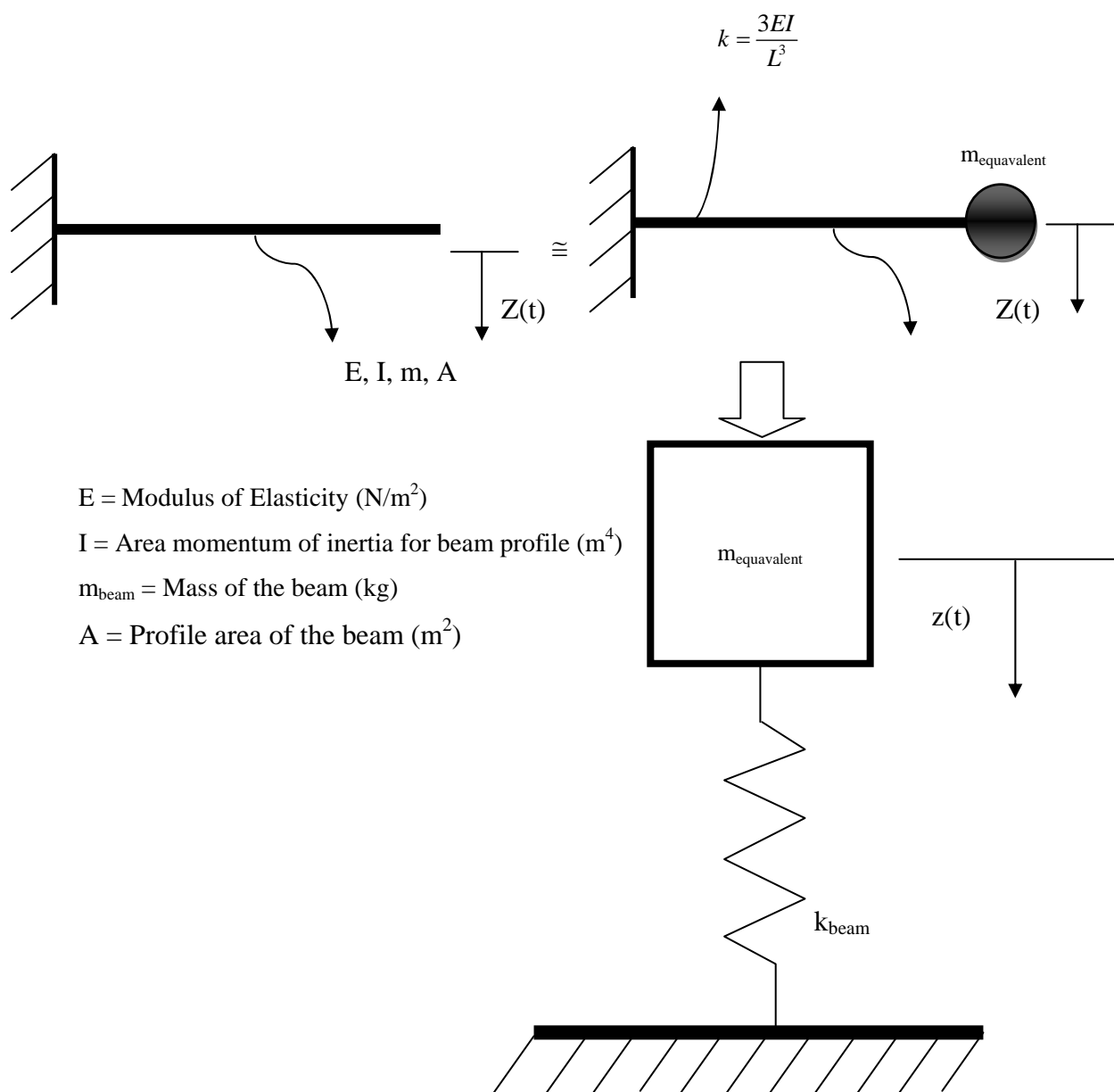


Figure 2.6 Equivalent beam model with single degree of freedom for embedded beam.

### 2.2.3 Natural Frequency Expression for an Embedded Beam: Distributed Parameter System Assumption:

Natural frequency of the embedded beam can be calculated more precisely with energy method. For a continuous system potential and kinetic energies of system can be shown as follows in accord with conservation of energy principle;

$$(E_K)_{MAX} + (E_P)_{MIN} = (E_K)_{MIN} + (E_P)_{MAX} \quad (2.8)$$

For an oscillating system when the kinetic energy of the system is at maximum the potential energy is zero. Similarly, when the potential energy is at maximum the kinetic energy is zero. Therefore, maximum kinetic energy and maximum potential energy of embedded beam are equal to one another.

$$(E_K)_{MAX} = (E_P)_{MIN} \quad (2.9)$$

Set of axes of the subject embedded beam as shown in Figure 2.10

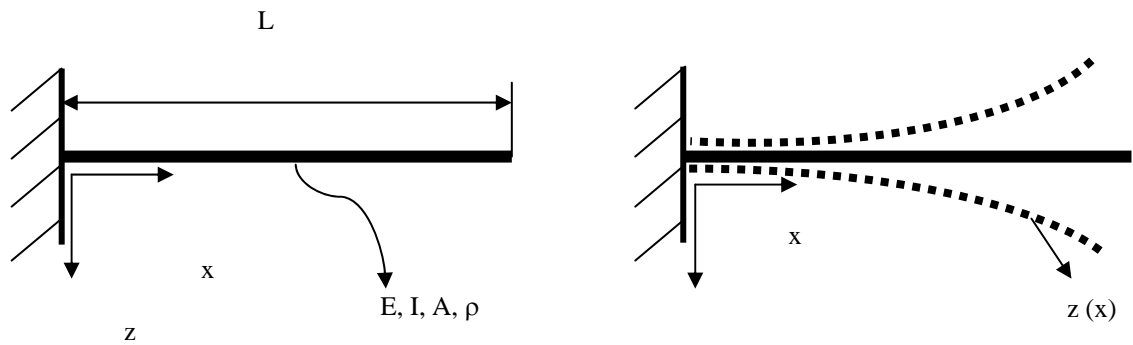


Figure 2.7 Embedded beam model and displacement graph.

Potential and kinetic energy expressions of uniform profile embedded beam can be given as follows;

$$E_p = \frac{1}{2} \int_0^L EI \left( \frac{d^2z}{dx^2} \right)^2 dx = \frac{1}{2} EI \int_0^L \left( \frac{d^2z}{dx^2} \right)^2 dx \quad (2.10)$$

$$E_k = \frac{1}{2} \int_0^L \rho A \left( \frac{dz}{dt} \right)^2 dx = \frac{1}{2} \rho A \int_0^L \left( \frac{dz}{dt} \right)^2 dx \quad (2.11)$$

The free vibration expression of embedded beam: is written as;

$$Z(t,x) = z(x) \sin \omega t \quad (2.12)$$

When used in potential and kinetic energy expressions

$$\frac{d^2 z}{dx^2} = \frac{d^2 Z}{dx^2} \sin \omega t, \frac{dz}{dt} = \omega Z \cos \omega t \quad (2.13)$$

When maximum values of potential and kinetic energy expressions are made equal:

$$\frac{1}{2} \int_0^L EI \left( \frac{d^2 Z}{dx^2} \sin \omega t \right)^2 dx = \frac{1}{2} \rho A \int_0^L (\omega Z \cos \omega t)^2 dx \quad (2.14)$$

Considering that the maximum value of sine and cosine expressions is 1 from here

$$\frac{1}{2} \int_0^L EI \left( \frac{d^2 Z}{dx^2} \right)^2 dx = \omega^2 \int_0^L \rho A Z^2 dx \quad (2.15)$$

expression is derived and natural frequency expression becomes

$$\omega_n^2 = \frac{\int_0^L EI \left( \frac{d^2 Z}{dx^2} \right)^2 dx}{\int_0^L \rho A Z^2 dx} \quad (2.16)$$

To derive the natural frequency expression displacement graph of embedded beam can be expressed as below as a fourth degree polynomial function of x. The displacement expression used must meet the limit conditions.

$$Z(x) = ax^4 + bx^3 + cx^2 + dx + e \quad (2.17)$$

Limit conditions for an embedded beam are as follows:

$$x = 0 \rightarrow Z(x=0) = 0 \text{ and } \frac{dZ}{dx} = 0, \quad x = L \rightarrow \frac{d^2Z}{dx^2} = 0 \text{ and } \frac{d^3Z}{dx^3} = 0 \quad (2.18)$$

Based on the limit conditions coefficients in the displacement graph can be found as:

$$b = -4aL, \quad c = 6aL^2, \quad d = 0, \quad e = 0 \quad (2.19)$$

When we place these coefficients in the equation (2.17), displacement graph of the beam can be expressed as:

$$Z(x) = a(x^2 - 4Lx^3 + 6L^2x^2) \quad (2.20)$$

This result can be used in frequency equation

$$\omega_n^2 = \frac{EI \int_0^L \left( \frac{d^2Z}{dx^2} \right) dx}{\rho A \int_0^L Z^2 dx} = \frac{EI \int_0^L \left( a(12x^2 - 24Lx^3 + 12L^2) \right)^2 dx}{\rho A \int_0^L \left( a(x^2 - 4Lx^3 + 6L^2x^2) \right)^2 dx} \quad (2.21)$$

When necessary integral calculations are made natural frequency expression of the embedded beam is found as:

$$\omega_n^2 = 12.4615 \frac{EI}{\rho AL^4} = 12.4615 \frac{EI}{mL^3} \rightarrow \omega_n = 3.530 \sqrt{\frac{EI}{mL^3}} \left( \frac{rad}{sn} \right) \quad (2.22)$$

When continuous system approach is used this frequency expression will provide a more precise result compared to the value derived based on assumption of system with single degree of freedom.

But to their different member configurations, robot manipulators have different positions in their operating envelope, and therefore they have varying rigidities. Considering the natural frequency formulation, due to varying rigidities of various

member positions in robot operating envelope will result in varying natural frequency values. In other words, a robot manipulator takes various rigidity values in its operating envelope and therefore varying natural frequencies, and shows varying vibration characteristic based on this. When we consider complex geometries of the robot members and assembly of robot manipulator model, it is not possible to use the method used above for an embedded beam to calculate natural frequency values of a robot manipulator system. In this study and dynamic behavior of the consider robot manipulators are computed by generating lumped parameter models of the robot manipulator and using the Finite Elements Method which enables numeric calculation of rigidity matrixes. SolidWorks simulation is used for numerical analyses. With finite elements method robot manipulator is modeled as a system with multiple degrees of freedom.

The finite elements model for robot manipulator is generated by using 4 node triangular prism elements with three degrees of transition freedom on each node. The finite element model used in the analyses as shown in Figure 2.8a and 2.8b. Finite elements model of manipulator consists of 36436 elements and 61500 nodes.



(a)

Figure 2.8

(a) Finite elements model of robot manipulator.

Mesh Details	
Study name	Study 2 (-AltPosition_Varsayilan_1-)
Mesh type	Solid Mesh
Mesher Used	Curvature based mesh
Jacobian points	4 points
Max Element Size	30 mm
Min Element Size	6 mm
Mesh quality	High
Total nodes	61500
Total elements	36436
Maximum Aspect Ratio	61.52
Percentage of elements with Aspect Ratio < 3	87.1
Percentage of elements with Aspect Ratio > 10	0.294
% of distorted elements (Jacobian)	0
Remesh failed parts with incompatible mesh	Off
Time to complete mesh(hh:mm:ss)	00:00:08

(b)

Figure 2.8b

(b) Finite element model of robot manipulator.

Using the finite element method, displacement equation of the continuous structure with  $n$  degrees of freedom under external excitation can be shown as follows in matrix form:

$$[M]\{\ddot{Z}\} + [k]\{Z\} = \{f\} \quad (2.23)$$

In this expression  $M$  indicates mass matrix of the structure,  $K$  indicates rigidity matrix of the structure and  $f$  indicates the external force affecting the structure. and  $z$  respectively indicates acceleration and displacement vectors of the nodes in the finite element model, respectively expression is valid for the static behavior of the structure:

$$[k]\{Z\} = \{f\} \quad (2.24)$$

Following matrix equation is used for the free vibration of the structure:

$$[M]\{\ddot{Z}\} + [K]\{Z\} = 0 \quad (2.25)$$



To calculate the natural frequency and related vibration modes the problem is turned into an eigen value problem on assumption of exponential response for displacement vector.

$$([K] - \omega^2 [M])\{z\} = 0 \quad (2.26)$$

The  $\omega$  here indicated the frequency vector comprising natural frequencies of the structure.  $Z$  indicates vibration mode vectors of these frequencies. Using computer assisted engineering software natural frequency values of structures with complex geometries and vibration modes showing how the structure vibrates on these frequencies can be found.

#### ***2.2.4 Different Studies on the Flexible Rotor Beam Element for the Manipulators with Joint and Link Flexibility.***

By Yue and Bai, this presented a new flexible rotor beam element to study the dynamic behaviour of manipulators with flexible links and joints. Both link and joint flexibility are incorporated together by using the finite model which is the combination of a finite element model for links and a torsional spring model for joints. The coupling terms of link and joint flexibility are considered in the dynamic equations of the manipulator. A planar 3R manipulator with flexible links and joints is analyzed as an example. The mathematical model used in the reference study is given in Figure 2.9.

The results of numerical simulation show the significant effect of joint flexibility on the dynamics of compliant manipulators.

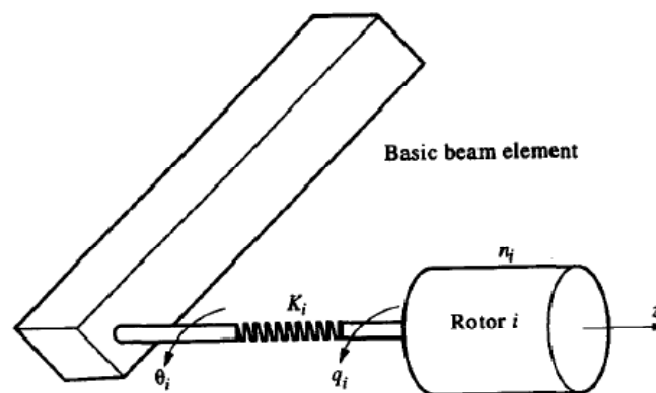


Figure 2.9 The flexible rotor beam element (Yue Shigang et al.)

### 2.2.5 Flexible Rotor Beam Element Model (studied by Yue and Bai )

In order to model the compliant manipulator, a new beam element, called the flexible rotor beam element, is proposed here to describe the link and joint flexibility at same time.

A flexible rotor beam element is the combination of a basic beam element and a rotor connected by a linear torsional spring, as shown in Figure 2.10, where  $\phi_i$  is the gear ratio of a gear unit at joint  $i$ ,  $\phi_{zi}$  is the moment of inertia of rotor  $i$  about its  $z$ -axis,  $\tau_i$  is the torque of  $i$ th rotor,  $q_i$  is the generalized coordinate for the  $i$ th rotor,  $\theta_i$  is the input angle of the  $i$ th link,  $\delta_i$  is the deformation of the  $i$ th torsional spring

$$\delta_i = q_i - \theta_i \quad (2.27)$$

The transverse deflections of a basic beam element are modeled by a quintic polynomial and the longitudinal deflections assumed to be a linear polynomial. The generalized coordinates of the element are assembled in a matrix form as

$$\{\phi\}_e = \{\phi_1 \ \phi_2 \ \phi_3, \dots \ \phi_8\} \quad (2.28)$$

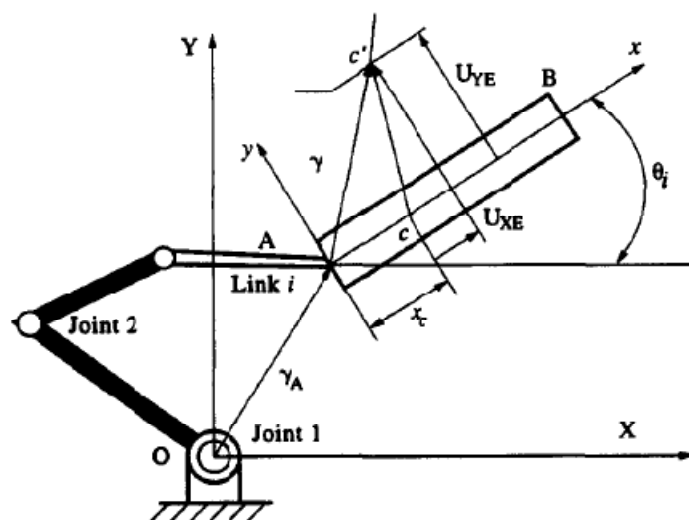


Figure 2.10 The deformations of an element in a flexible manipulator.(Yue Shigang et al)

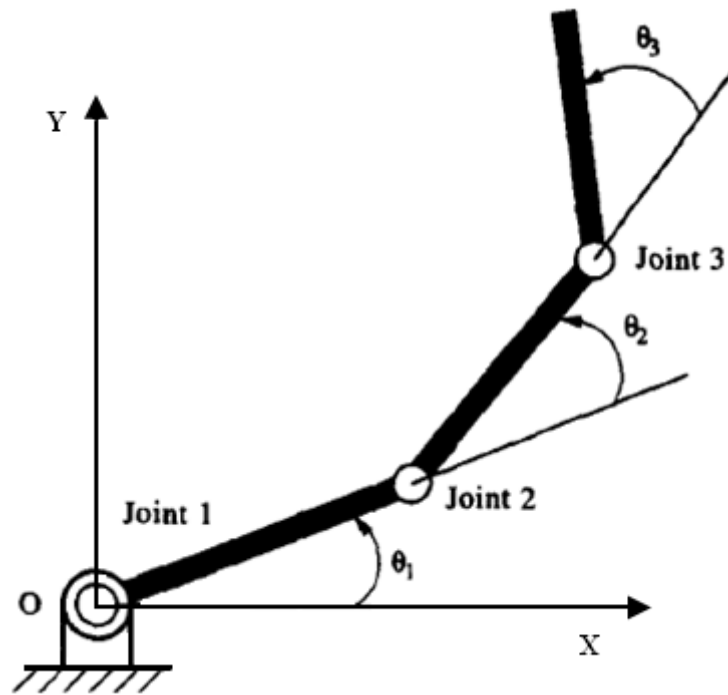


Figure 2.11 A planar 3R manipulator (Yue Shigang et al)

The transverse deformation  $U_{YE}$  and the longitudinal deformation  $U_{XE}$  as shown in Figure 2.13 of an arbitrary point  $c$  at the  $x$  axis of a element can be expressed as follows:

$$U_{YE} = \{\phi\}_e^T \{D_Y\} \quad (2.29)$$

$$U_{XE} = \{\phi\}_e^T \{D_X\} \quad (2.30)$$

where  $\{D_Y\}$  and  $\{D_X\}$  are the vectors of the interpolation polynomials. Before the dynamic equation can be obtained, it is necessary to derive the kinetic and potential energy of the element.

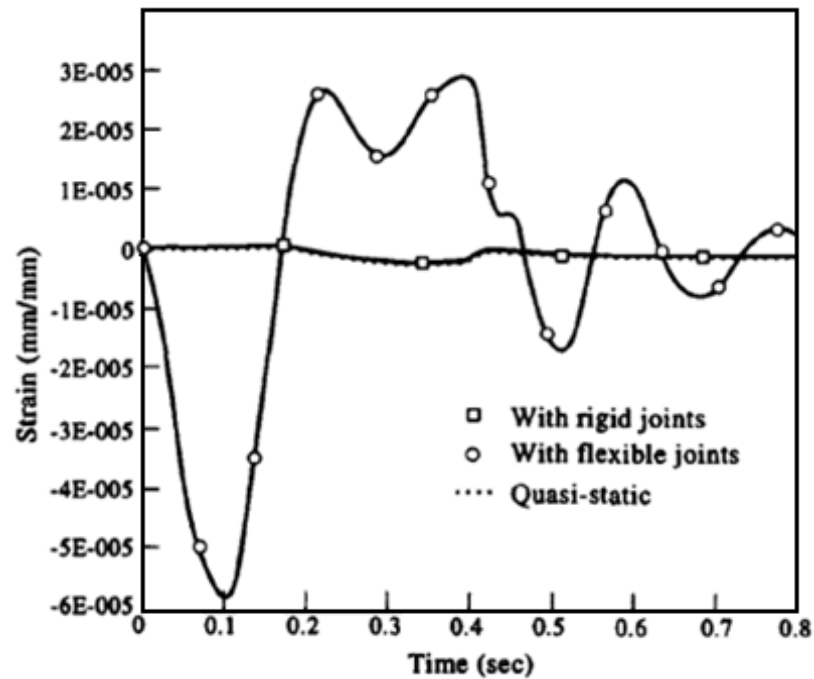


Figure 2.12 The base joint strain. (Yue Shingang et al)

According to the results given in this reference work, a new flexible rotor beam element has been developed to study dynamic behaviour of planar manipulators with flexible links and joints. The joint compliance and link flexibility have been considered simultaneously. The results from the numerical simulation of a planar 3R manipulator show that joint flexibility plays a significant role in the dynamic behaviour of flexible manipulator and should therefore be considered, in addition to link elasticity, in the design and control of compliant manipulators.

## CHAPTER THREE

### TECHNICAL DATA OF THE ROBOT

#### 3.1 Technical Data of the Robot

In this study (Cincinnati-Milacron) robot is considered for frequency analysis. Staubli robot weighs 721 kg and has a payload capacity of 30 kg. Operating envelope as shown in Figure 3.1 and 3.2. Data on movements in operating envelope is shown on Table 3.1 Highest Cartesian speed of the manipulator is 1.5 m/sec. Finally, angular velocity, oscillation and angular resolution of each joint as shown in Table 3.2 and Figure 3.3.

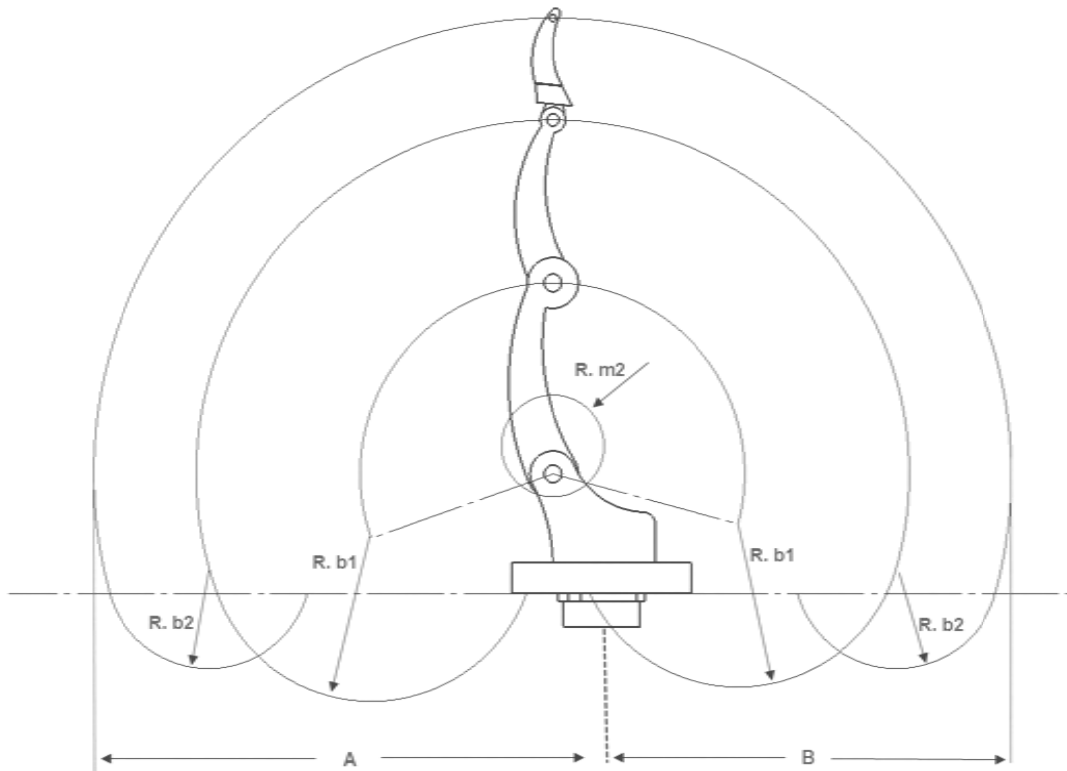


Figure 3.1 Frontal view of robot. All values on the figure are also given on Table 2.1

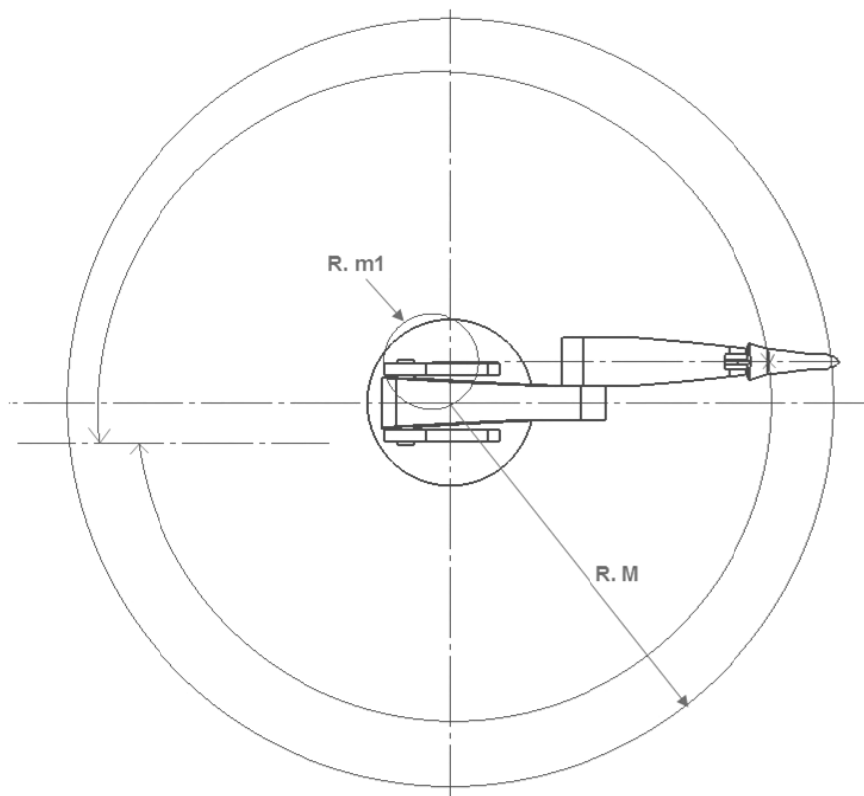


Figure 3.2 Top view of robot. All values on the figure are also given on Table 3.1

Table 3.1 Data on movements of robot in operating envelope.

R.M, maximum accessible distance between joint 1 and 5	3233 mm
R.m1, minimum accessible distance between joint 1 and 5	401 mm
R.m2, minimum accessible distance between joint 2 and 5	400 mm
A	1980 mm
B	1600 mm
Repeatability under constant temperature	640 mm
R.b, distance between joint 3 and 5	400 mm

Table 3.2a Angular values of the joints of robot

Joint	1	2	3	4	5
Amplitude	360°	220°	290°	150°	540°
Operating angle distribution	±180°	±110	±145°	±75°	±270°

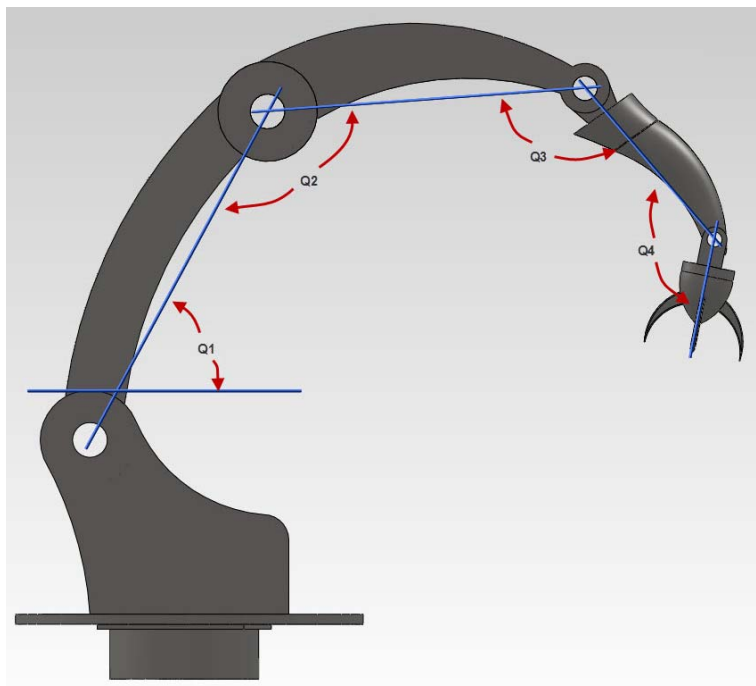


Figure 3.3 Angular values of the joints of robot

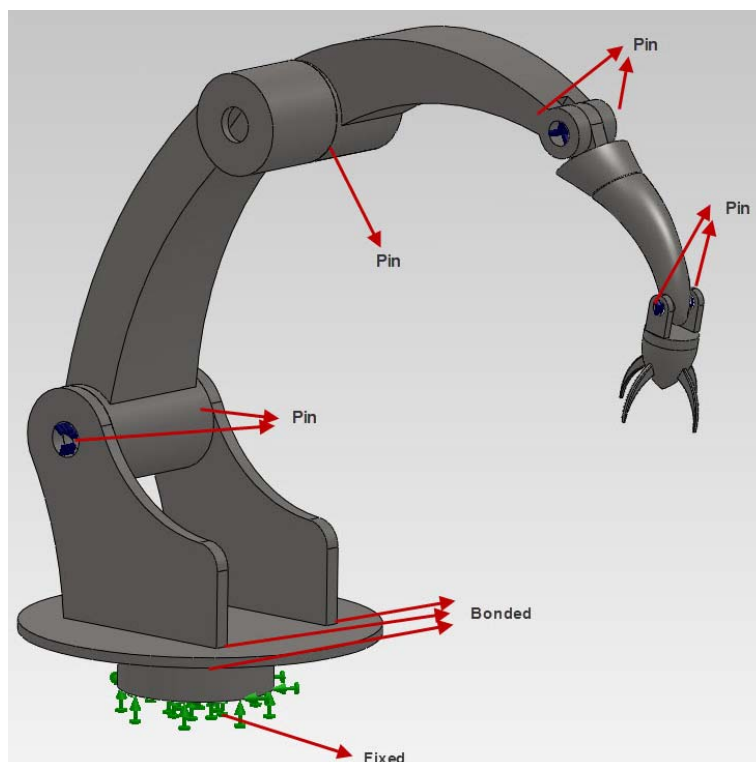


Figure 3.4 Description for Modified Cincinnati Milacron Robot arm

### **3.2 Kinematic Analysis**

Serial manipulators are connected to each other with various types of joints. One end of the manipulator is fixed onto the ground, while the other end freely moves in space. Therefore serial manipulators are sometimes called open loop manipulators. Fixed member is called the support, and the free end used for mechanical gripper attachment is called end effector.

For specific tasks of the robots, the initial step is to determine the position of end effector relative to the support. This is called position analysis. There are two types of position analysis problems: direct kinematic and reverse kinematic. In direct kinematic displacement or rotation data are input and end effector position is output. In reverse kinematic, end effector position is the input and the output is displacement or rotation data.

### **3.3 Rigidity Analysis in Serial Manipulators**

When the manipulator carries out its programmed tasks, the end effector applies some forces and momenta on its environment. These contact forces and momenta causes end effector to deviate from the intended position. The degree of deviation is a function of the force applied to the manipulators and their rigidity. This manipulator rigidity has a direct effect on precise positioning. Furthermore, in some advanced control system, rigidity characteristic is used as feedback in robots. The rigidity of manipulators is based on the dimensions of the material used for the members, the mechanical transmission elements, the mechanisms, the controller and the actuator elements.

### **3.4 Rigidity Analysis in Serial Manipulators**

When the manipulator carries out its programmed tasks, end effector applies some forces and momenta on its environment. These contact forces and momenta causes end effector to deviate from the intended position. The degree of deviation is a function of the force applied to the manipulators and their rigidity. This manipulator



rigidity has a direct effect on precise positioning. Furthermore, in some advanced control system, rigidity characteristic is used as feedback in robots. The rigidity of manipulators is based on the dimensions of the material used for the members, the mechanical transmission elements, the mechanisms, the controller and the actuator elements.

# CHAPTER FOUR

## THE NATURAL FREQUENCY ANALYSIS

### 4.1 The Natural Frequency Analysis of the Aluminum beam

Analyses were conducted with 10 degree increments from 0 to 90 degrees for first robot arm and with 10 degree increments from 0 to 180 degrees. In other words natural frequency analyses were conducted for 190 degrees different positions. In our analyses we selected to use aluminum pins. As shown in Figures 4.1, 4.2 and 4.3 when the big arm  $\phi_1$  is  $0^\circ$  and the angular position of the small arm  $\phi_2$  takes valve changes between ( $0^\circ$ ,  $60^\circ$  and  $180^\circ$ ).

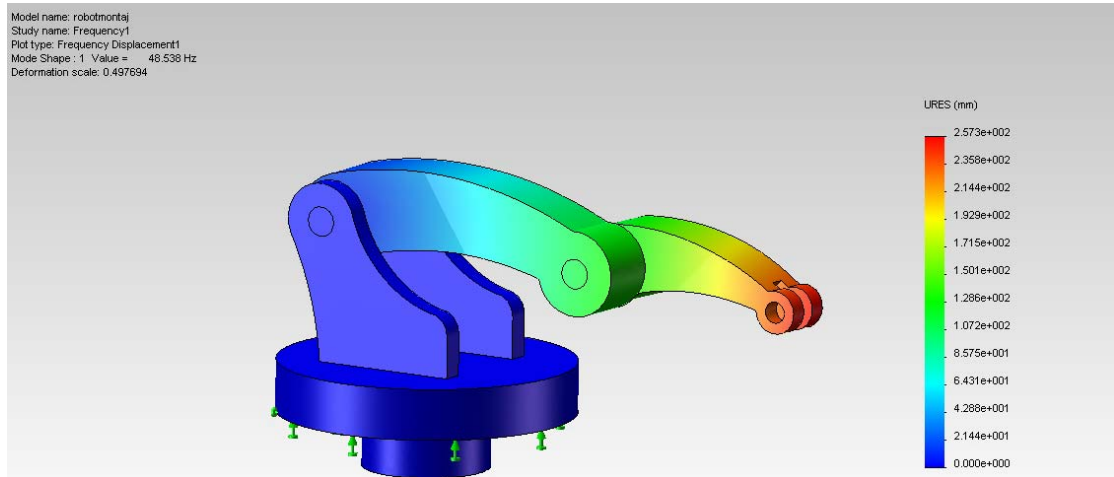


Figure 4.1 The joint angle of the big arm  $\phi_1$  is  $0^\circ$  and the small arm  $\phi_2$  is  $0^\circ$

In this position the natural frequency is 48.538 Hz.

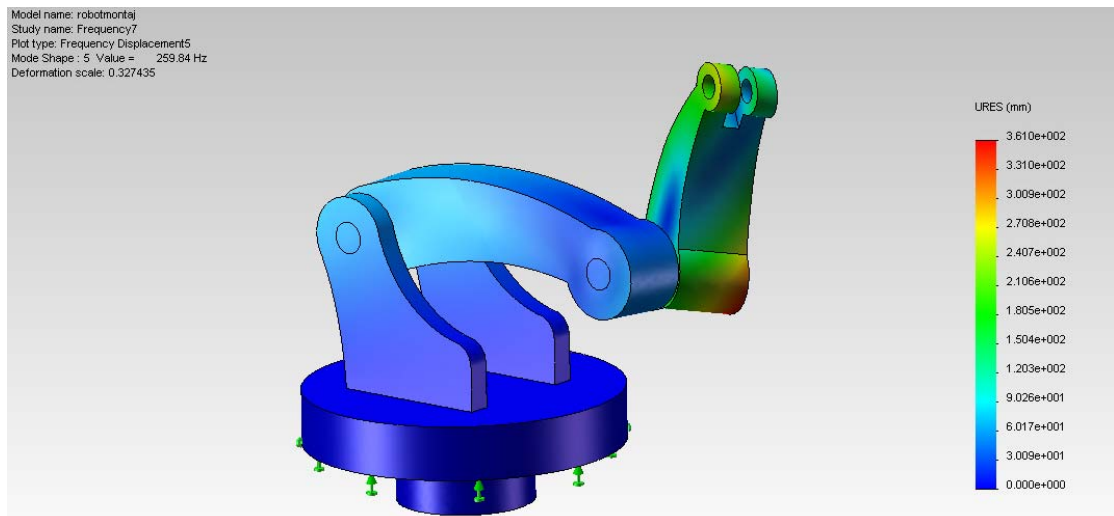


Figure 4.2 The joint angle of the big arm  $\phi_1$  is  $0^\circ$  and the small arm  $\phi_2$  is  $60^\circ$

In this position natural frequency is 259.84 Hz.

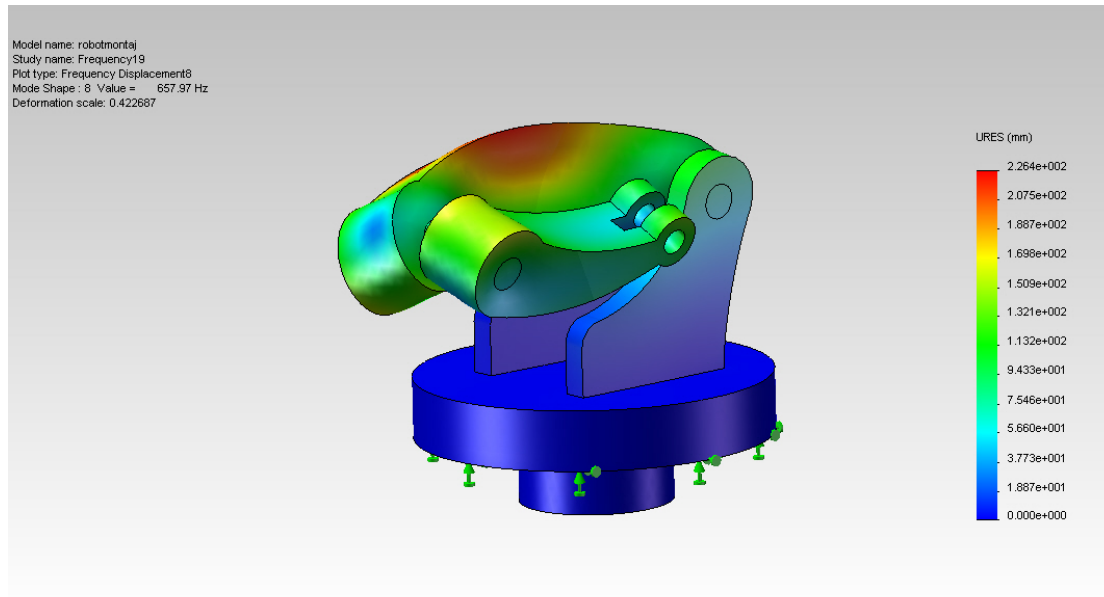


Figure 4.3 The joint angle of the big arm  $\varnothing_1$  is  $0^\circ$  and the small arm  $\varnothing_2$  is  $180^\circ$

In this position the natural frequency is 657.97 Hz.

On our analysis selected to use aluminum pins, as shown in Figures 4.4 and 4.5 when the big arm  $\varnothing_1$  is  $60^\circ$  and the angular position of the small arm  $\varnothing_2$  takes valve changes between ( $0^\circ$  and  $180^\circ$ ).

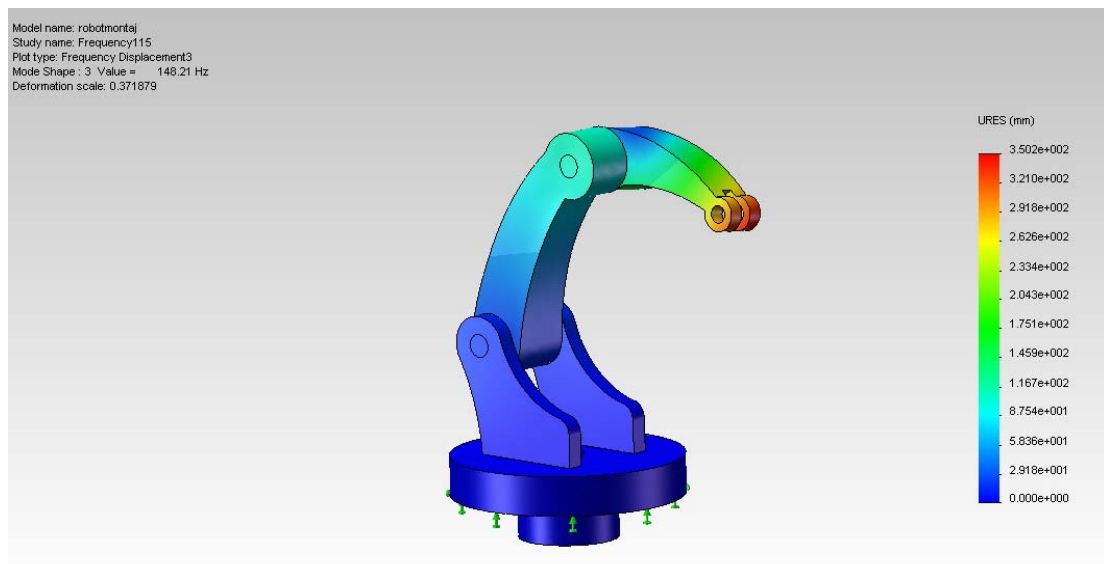


Figure 4.4 The joint angle of the big arm  $\varnothing_1$  is  $60^\circ$  and the small arm  $\varnothing_2$  is  $0^\circ$

In this position the natural frequency is 147.21 Hz.

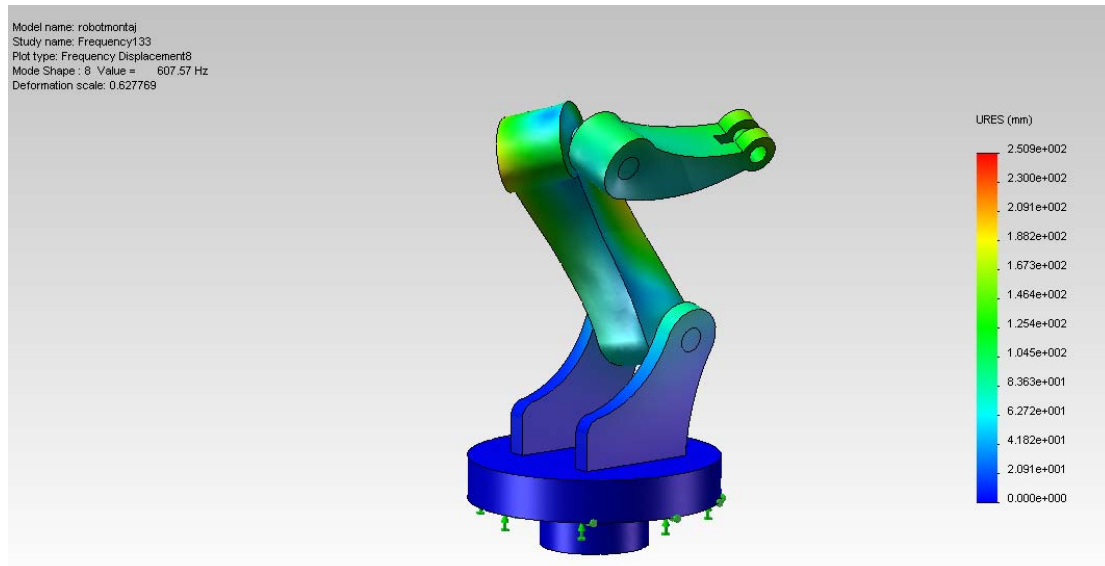


Figure 4.5 The joint angle of the big arm  $\phi_1$  is  $60^\circ$  and the small arm  $\phi_2$  is  $180^\circ$

In this position the natural frequency is 607.57 Hz.

Finally, on our analyses selected to use aluminum pins. As shown in Figures 4.6 and 4.7 when the big arm  $\phi_1$  is  $90^\circ$  and the angular position of the small arm  $\phi_2$  takes value changes between ( $90^\circ$  and  $180^\circ$ ).

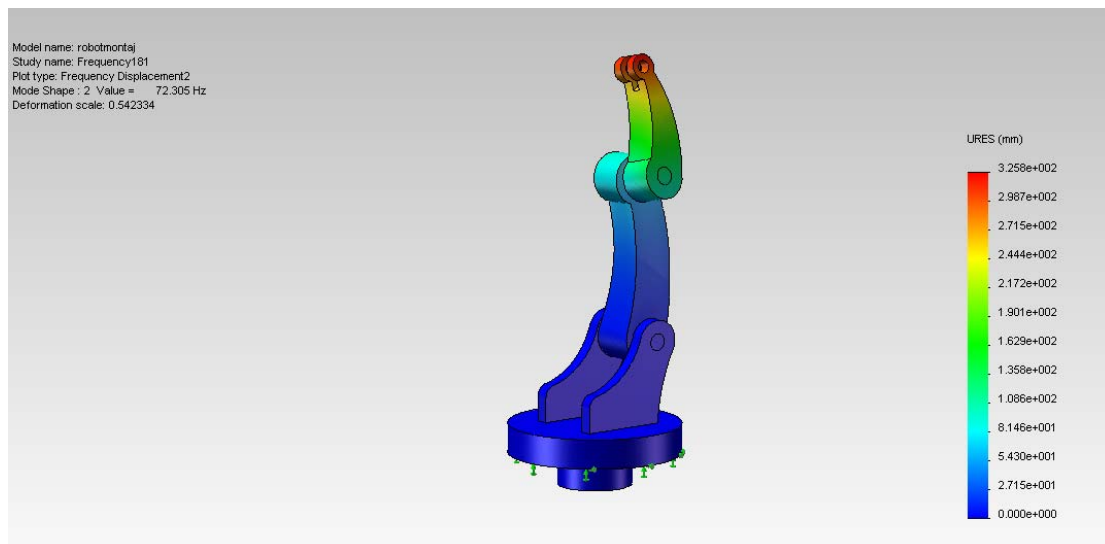


Figure 4.6 The joint angle of the big arm  $\phi_1$  is  $90^\circ$  and the small arm  $\phi_2$  is  $90^\circ$

In this position the natural frequency is 72.305 Hz, as shown in Figure 4.6.

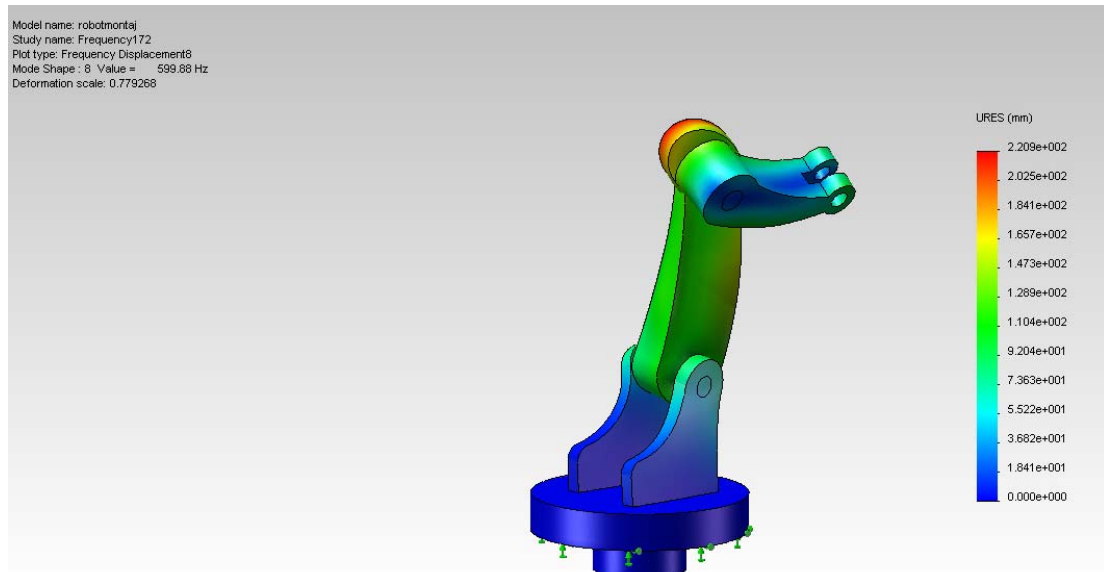


Figure 4.7 The joint angle of the big arm  $\phi_1$  is  $90^\circ$  and the small arm  $\phi_2$  is  $180^\circ$

In this position the natural frequency is 599.88 Hz.

In the five frequency spectra below that made with MATLAB programme, we can see clearly the different in natural frequencies values. As shown in Figures 4.8, 4.9, 4.10, 4.11, 4.12 and 4.13.

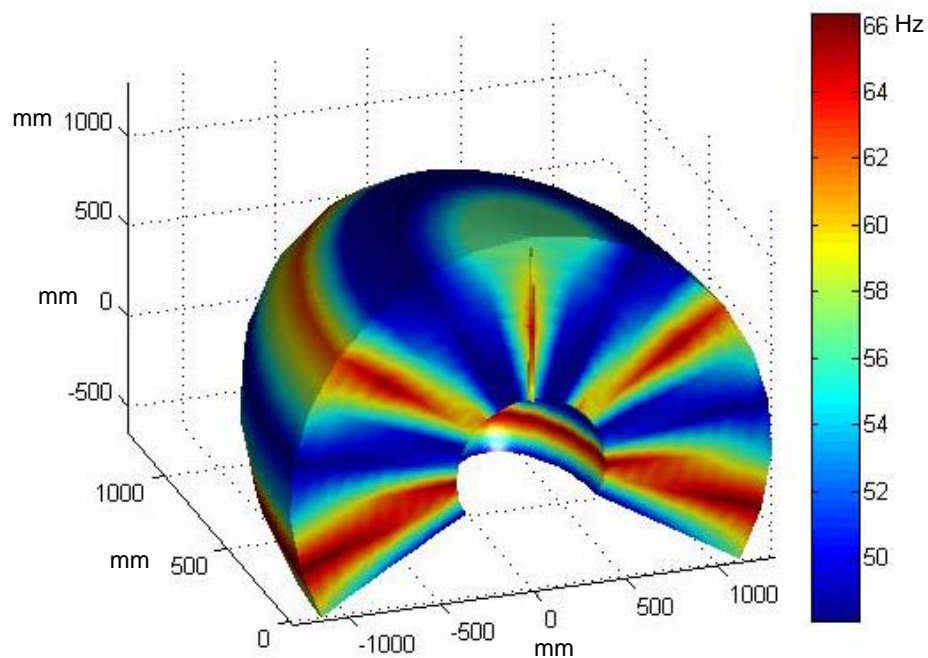


Figure 4.8 The workspace graphic for the first frequency

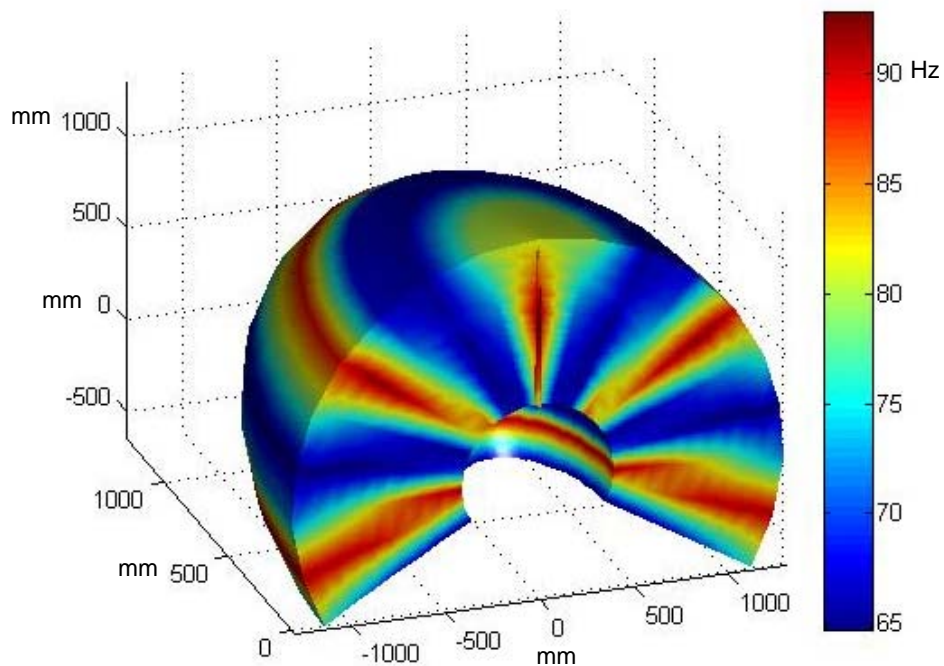


Figure 4.9 The workspace graphic for the second frequency

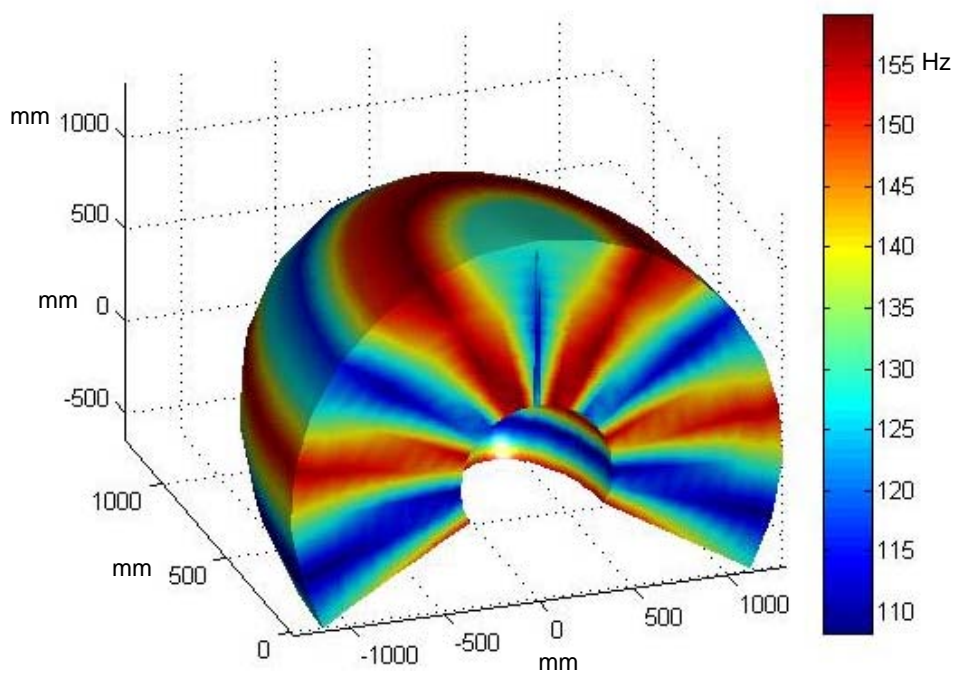


Figure 4.10 The workspace graphic for the third frequency

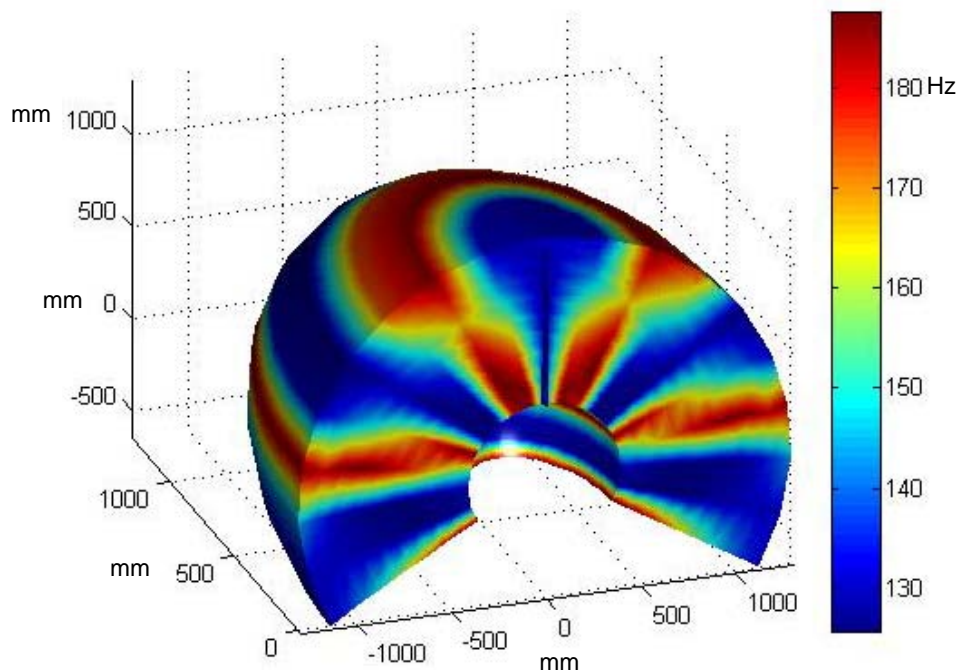


Figure 4.11 The workspace graphic for the fourth frequency

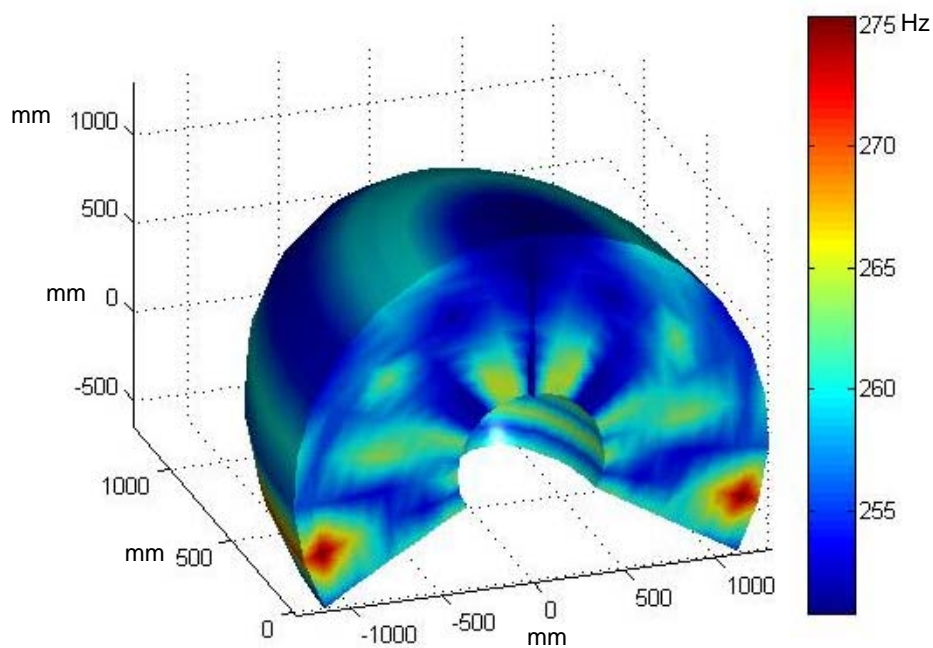


Figure 4.12 The workspace graphic for the fifth frequency

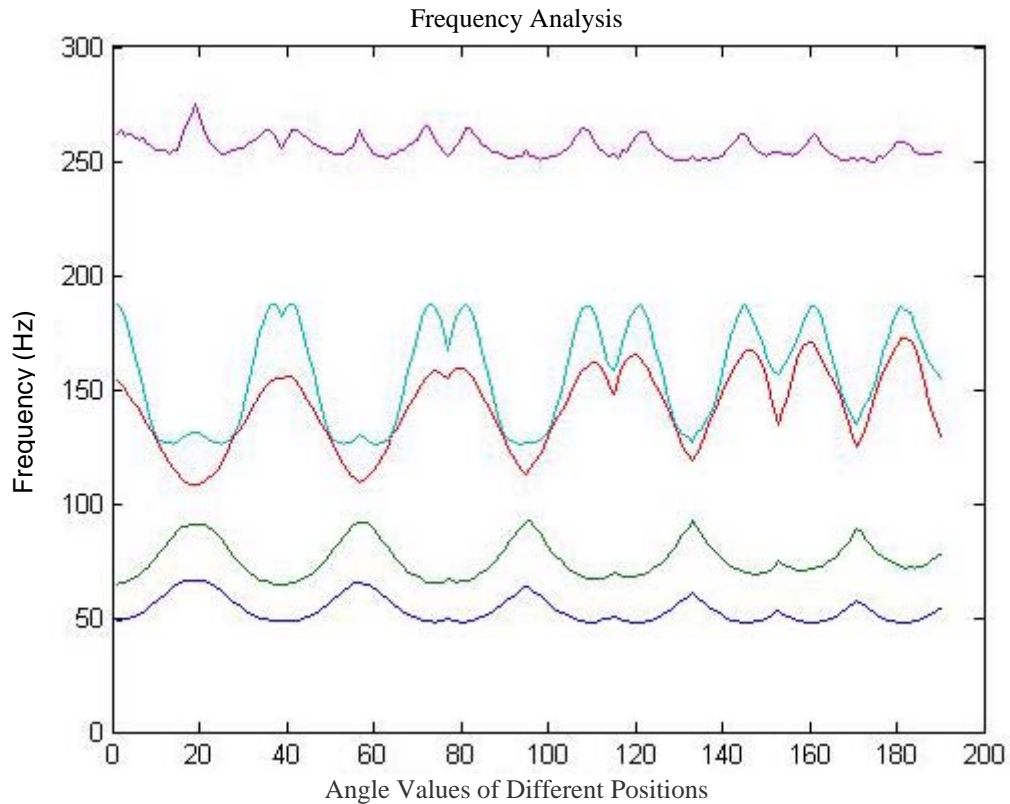


Figure 4.13 The diagram for the five different frequency positions

We can see from the workspace graphics, when we used aluminum materials in the analyses, it has been observed that the aluminum materials exhibits rigid pattern during the movement of the manipulator.

#### 4.2 The Natural Frequency Analysis of the Steel Manipulator

Analyses were conducted with 10 degree increments from 0 to 90 degrees for first robot arm and with 10 degree increments from 0 to 180 degrees. In other words natural frequency analyses were conducted for 190 degrees different positions. In our analyses we selected to use steel pins, as shown in Figures 4.14 and 4.15 when the big arm angle  $\phi_1$  is  $0^\circ$  and the angular position of the small arm  $\phi_2$  changes between ( $0^\circ$  and  $180^\circ$ ).



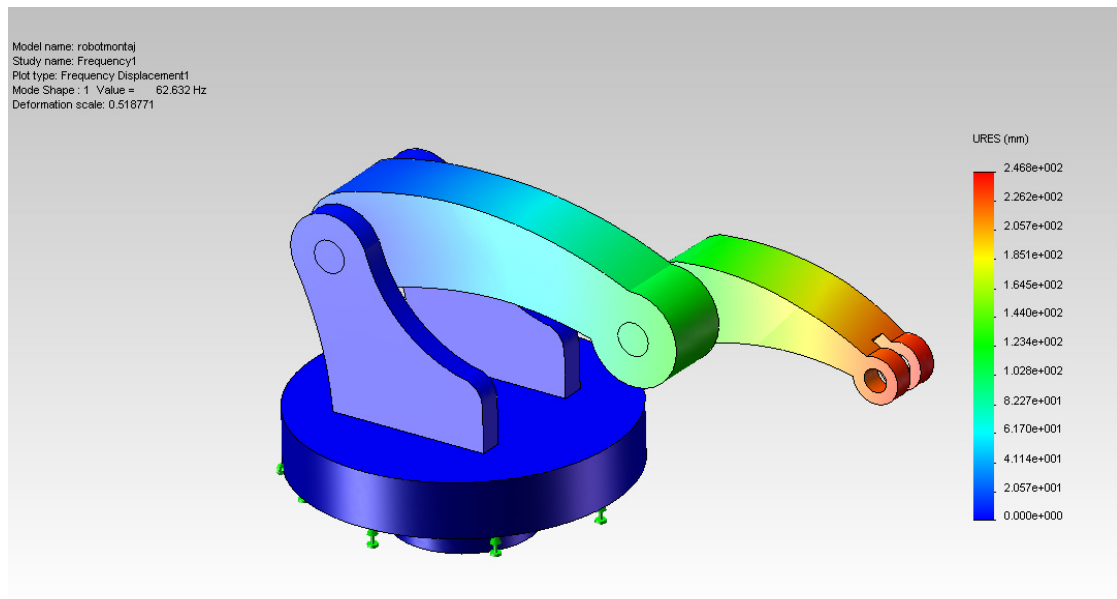


Figure 4.14 The joint angle of the big arm  $\phi_1$  is  $0^\circ$  and the small arm  $\phi_2$  is  $0^\circ$

In this position the natural frequency is 62.632 Hz,

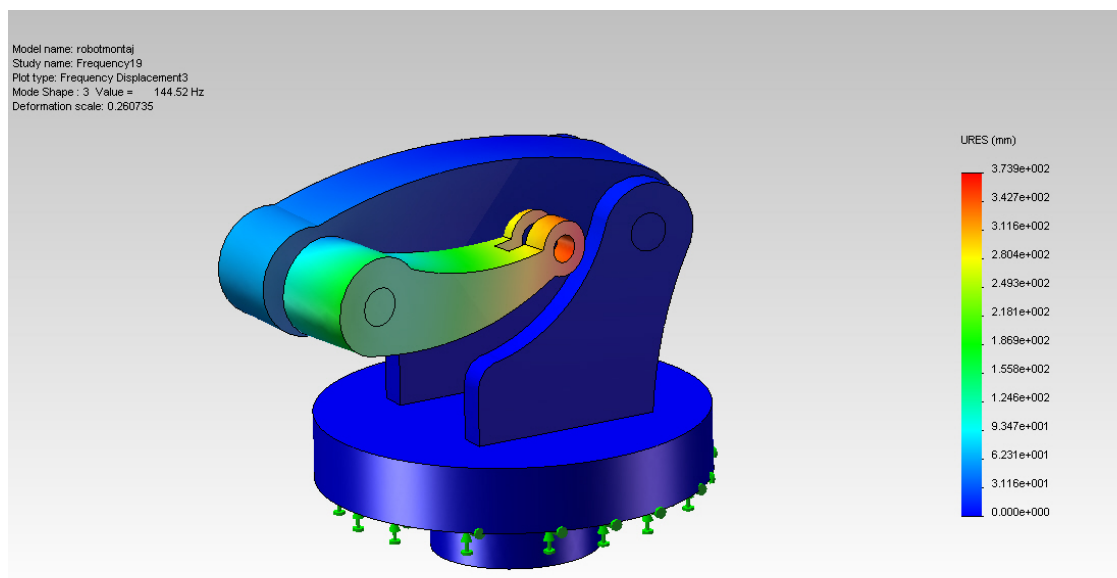


Figure 4.15 The joint angle of the big arm  $\phi_1$  is  $0^\circ$  and the small arm  $\phi_2$  is  $180^\circ$

In this position the natural frequency is 144.52 Hz, as shown in Figure 4.15.

For our analysis we selected to use steel pins. As shown in Figures 4.16 and 4.17 when the big arm angle  $\phi_1$  is  $60^\circ$  and the angular position of the small arm  $\phi_2$  takes value ( $0^\circ$  and  $180^\circ$ ).

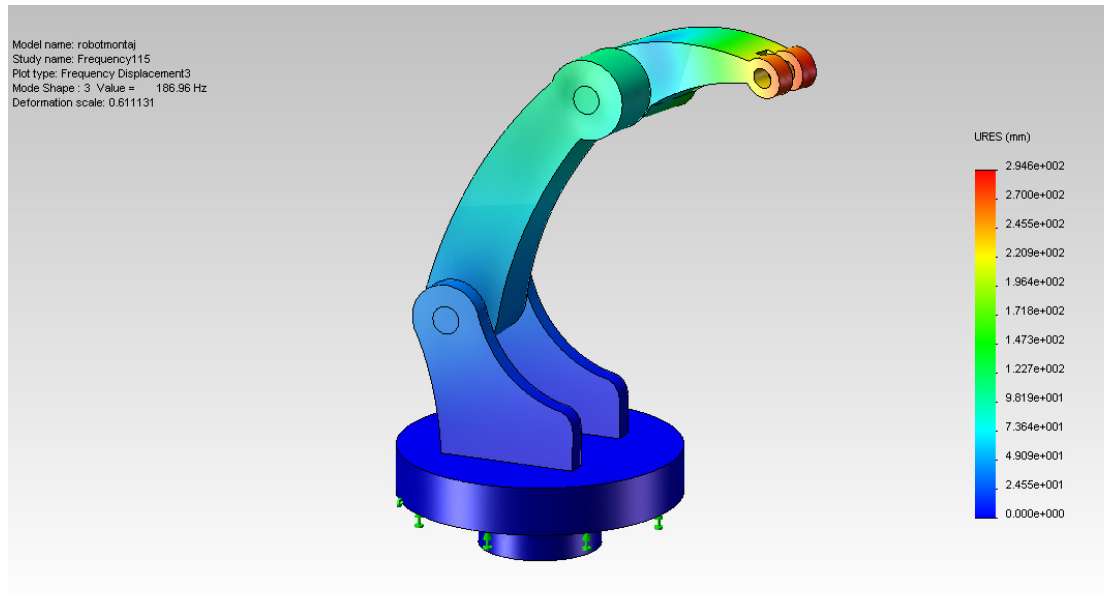


Figure 4.16 The joint angle of the big arm  $\varnothing_1$  is  $60^\circ$  and the small arm  $\varnothing_2$  is  $0^\circ$

In this position the natural frequency is 168.96 Hz.

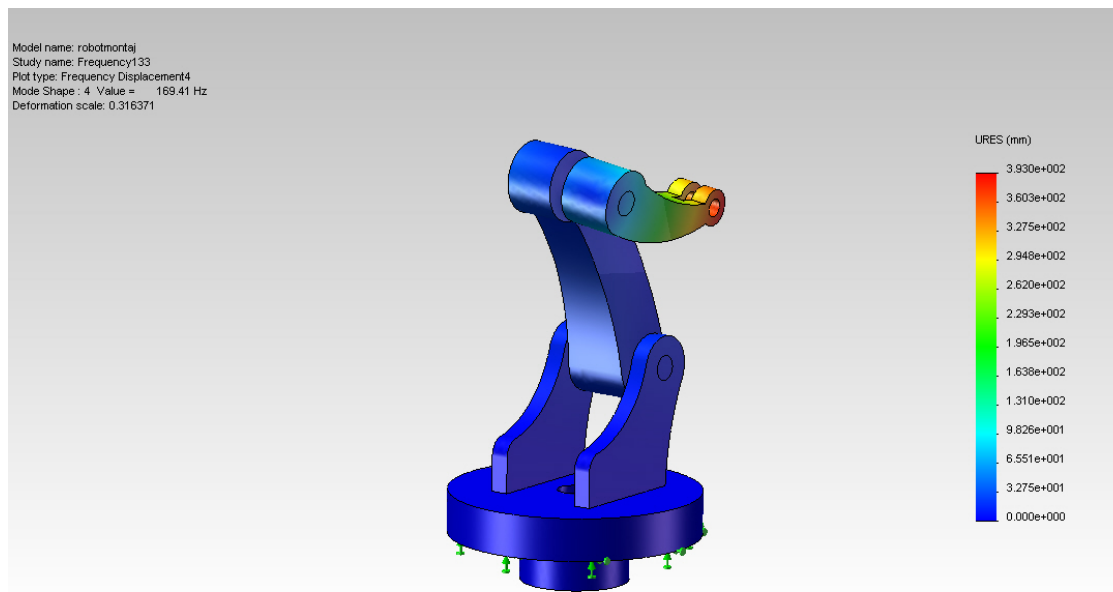


Figure 4.17 The joint angle of the big arm  $\varnothing_1$  is  $60^\circ$  and the small arm  $\varnothing_2$  is  $180^\circ$

In this position the natural frequency is 169.41 Hz

Finally, for our analysis selected to use steel pins, as shown in Figures 4.18 and 4.19 when the big arm angle  $\varnothing_1$  is  $90^\circ$  and the angular position of the small arm  $\varnothing_2$  takes value ( $90^\circ$  and  $180^\circ$ ).

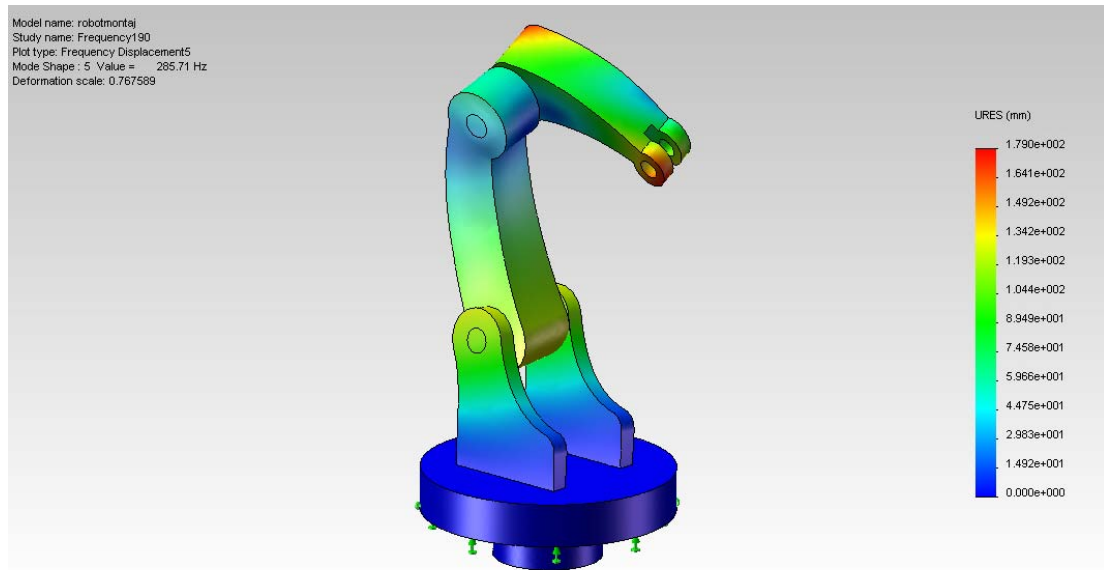


Figure 4.18 The joint angle of the big arm  $\phi_1$  is  $90^\circ$  and the small arm  $\phi_2$  is  $90^\circ$

In this position the natural frequency is 285.71 Hz

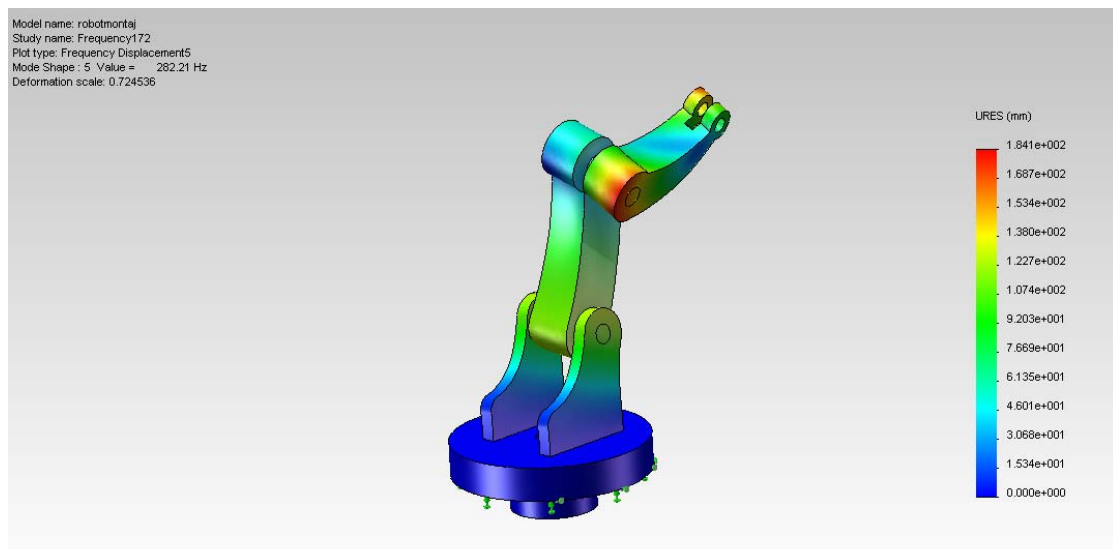


Figure 4.19 The joint angle of the big arm  $\phi_1$  is  $90^\circ$  and the small arm  $\phi_2$  is  $180^\circ$

In this position the natural frequency is 282.21 Hz

In the five frequency spectra below that made with MATLAB programme, we can see clearly the difference in natural frequencies values when we use steel material. As shown in Figures 4.20, 4.21, 4.22, 4.23, 4.24 and 4.25.

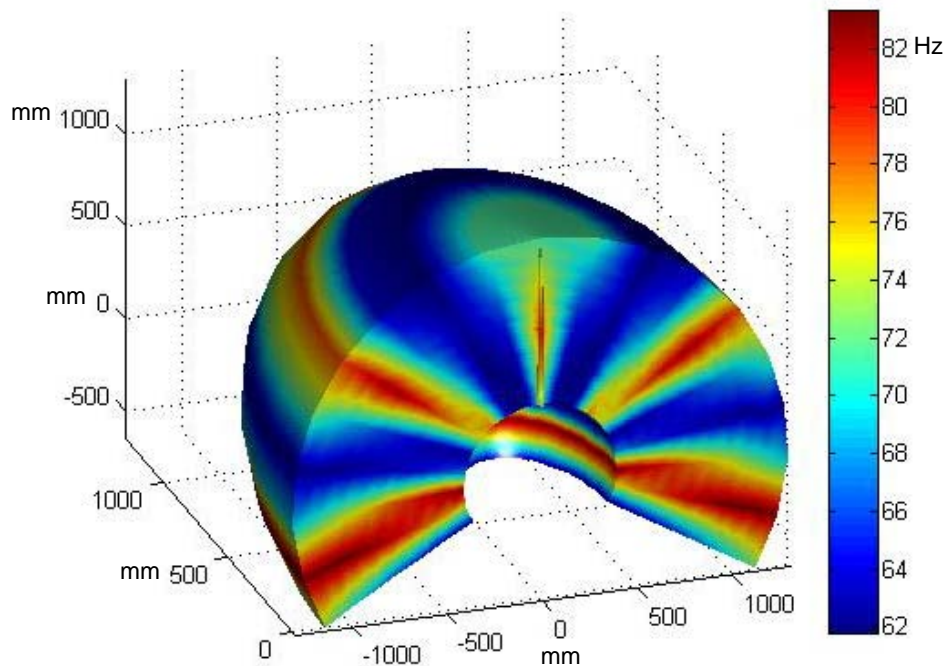


Figure 4.20 The workspace graphic for the first frequency

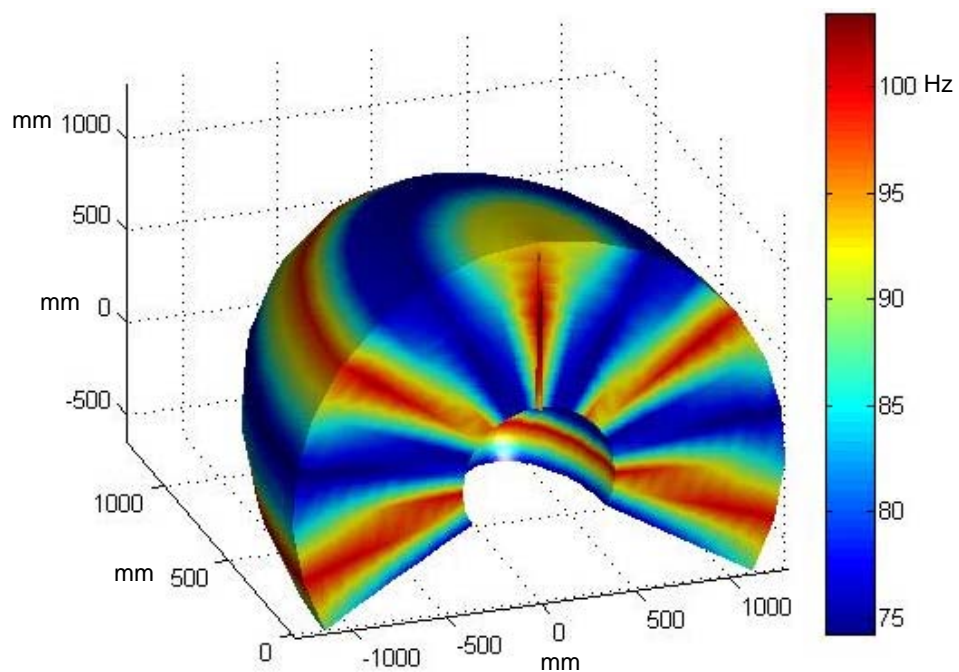


Figure 4.21 The workspace graphic for the second frequency

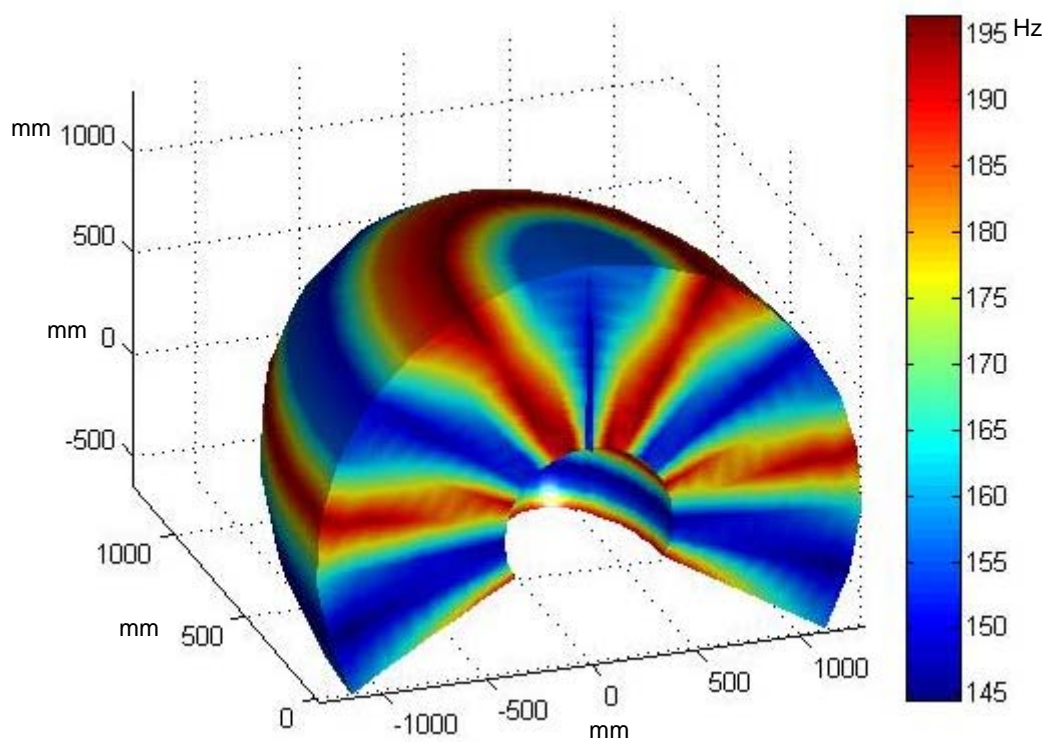


Figure 4.22 The workspace graphic for the third frequency

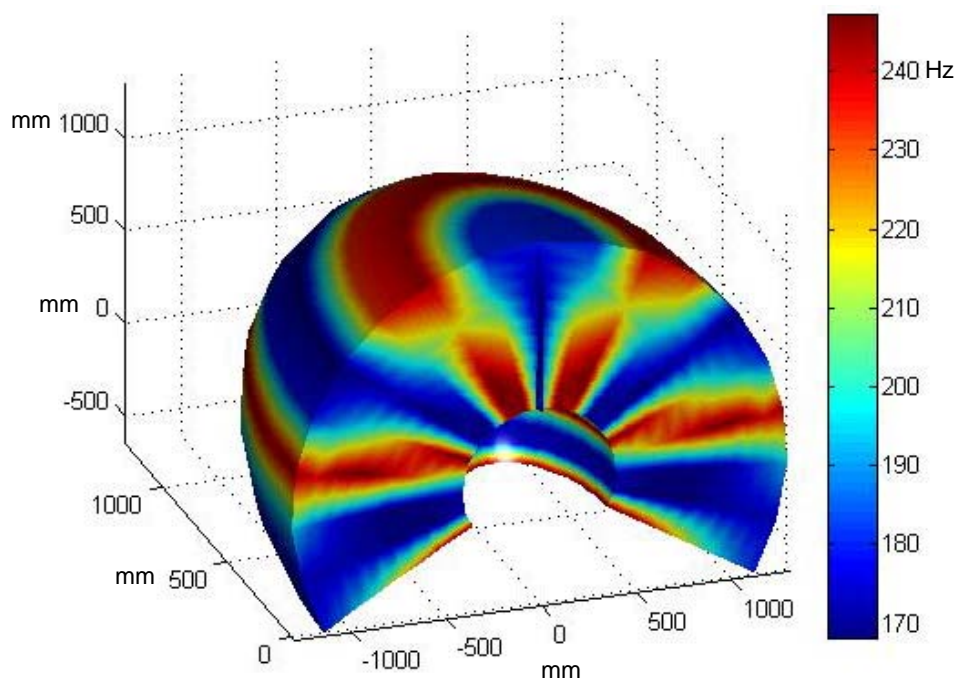


Figure 4.23 The workspace graphic for the fourth frequency

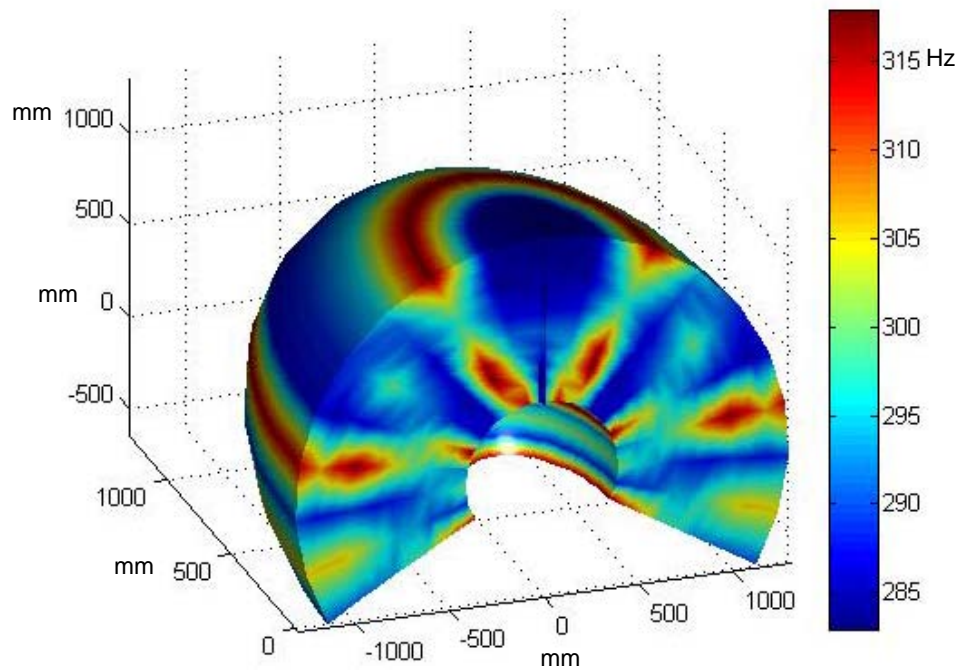


Figure 4.24 The workspace graphic for the fifth frequency

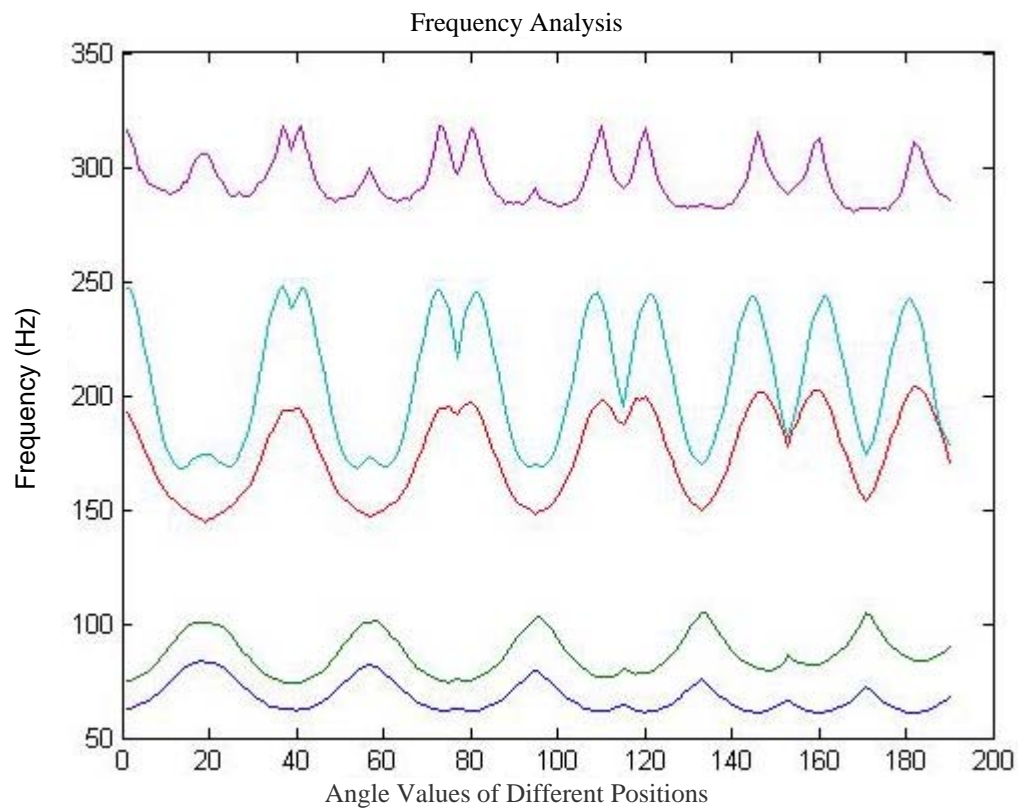


Figure 4.25 The diagram for the five different frequency positions for steel

We can see from the workspace graphics that the steel material exhibits a more rigiditive pattern during the movement of the manipulator.

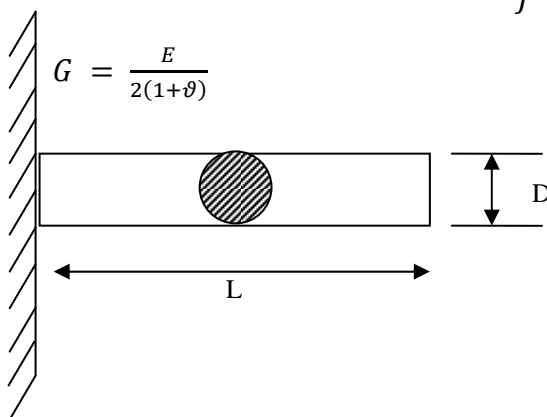
### 4.3 Examine The Effect of The Equivalent Arc Parameters to the Flexibility of the System By Utilizing From The Pin Connector Feature of the Solidworks Programme.

#### 4.3.1 Torsion Spring Coefficient Calculation for the Aluminum Material:

The equivalent spring coefficient for a torsional spring in the form a cylindrical rod;

$$K_{\theta} = \frac{GxJ_P}{L}$$

$$J = \frac{\pi x D^4}{32}$$



$\nu$  is poisson ratio

$G$  is shear modulus

$J$  is polar moment of inertia

$L$  : 330 mm = 0,33 m,

$D$  : 70 mm = 0,07 m

$$G = \frac{6.9 \times 10^{10}}{2(1 + 0,33)} = 2.593984 \times 10^{10}$$

$$J = \frac{\pi \times 0,07^4}{32} = 2.35598125 \times 10^{-6}$$

$$K_{\theta} = \frac{2.593984 \times 10^{10} \times 2.35598125 \times 10^{-6}}{0,33} = 185193.24 \text{ N.m/rad}$$

We used this result in our analysis which we selected to use the pin Connector feature of the Solidworks programme. As shown in Figures 4.26 and 4.27 when the big arm angle  $\phi_1$  is  $0^\circ$  and the angular position of the small arm  $\phi_2$  takes value ( $0^\circ$  and  $90^\circ$ ).

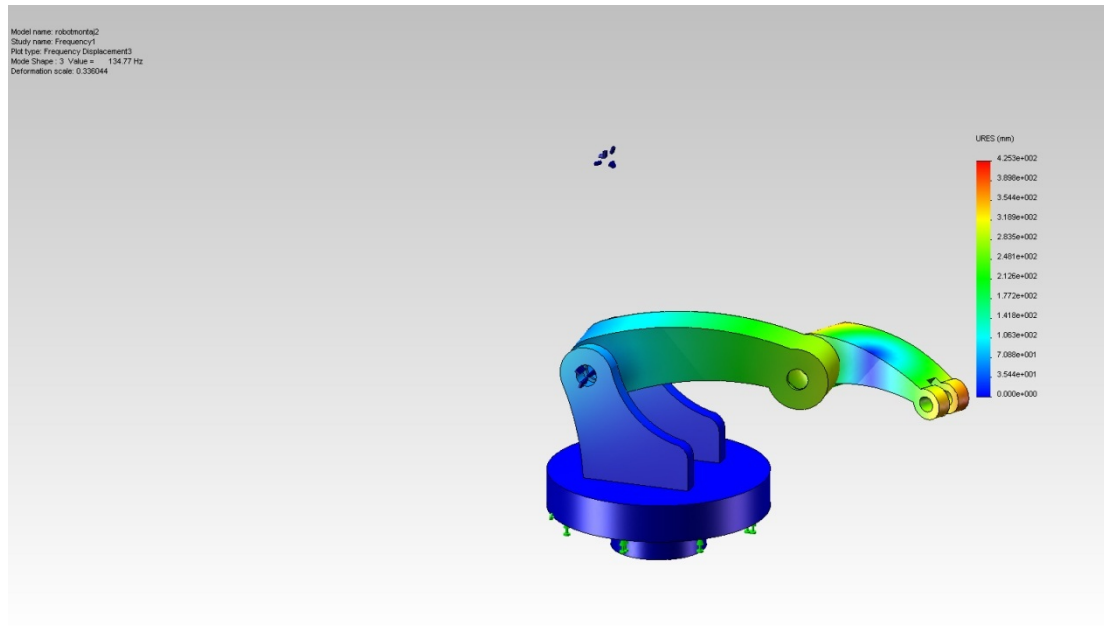


Figure 4.26 The joint angle of the big arm  $\phi_1$  is  $0^\circ$  and the small arm  $\phi_2$  is  $0^\circ$

In this position the natural frequency is 134.77 Hz.

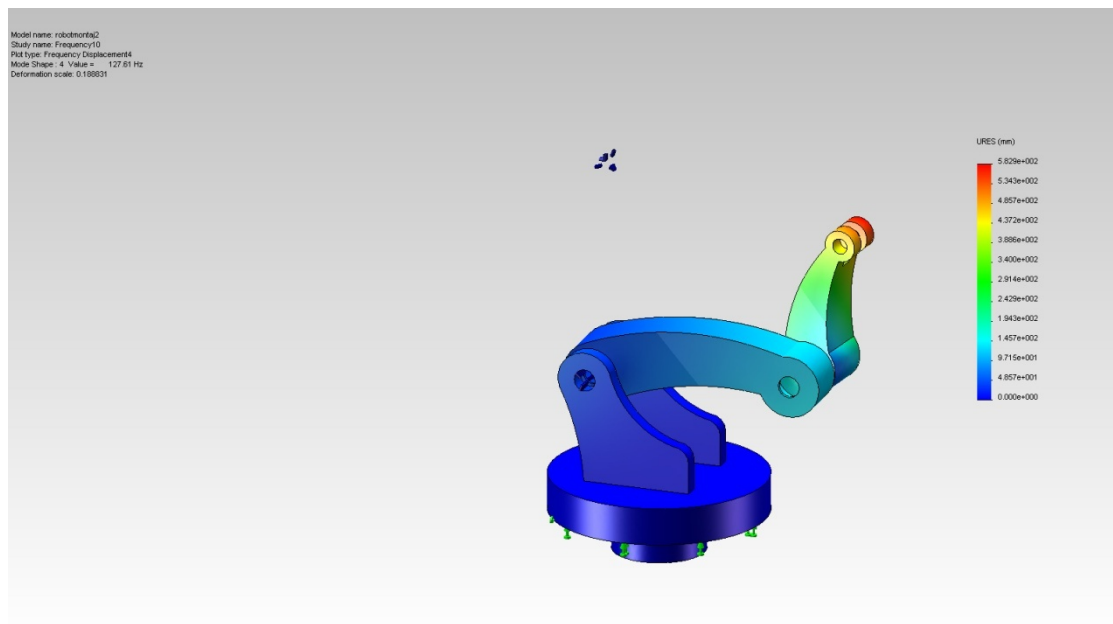


Figure 4.27 The joint angle of the big arm  $\phi_1$  is  $0^\circ$  and the small arm  $\phi_2$  is  $90^\circ$

In this position the natural frequency is 127.61 Hz

Finally, for our analysis we selected to use the pin Connector feature of the Solidworks program. As shown in Figures 4.28 and 4.29 when the big arm angle  $\phi_1$  is  $90^\circ$  and the angular position of the small arm  $\phi_2$  takes value ( $0^\circ$  and  $90^\circ$ ).



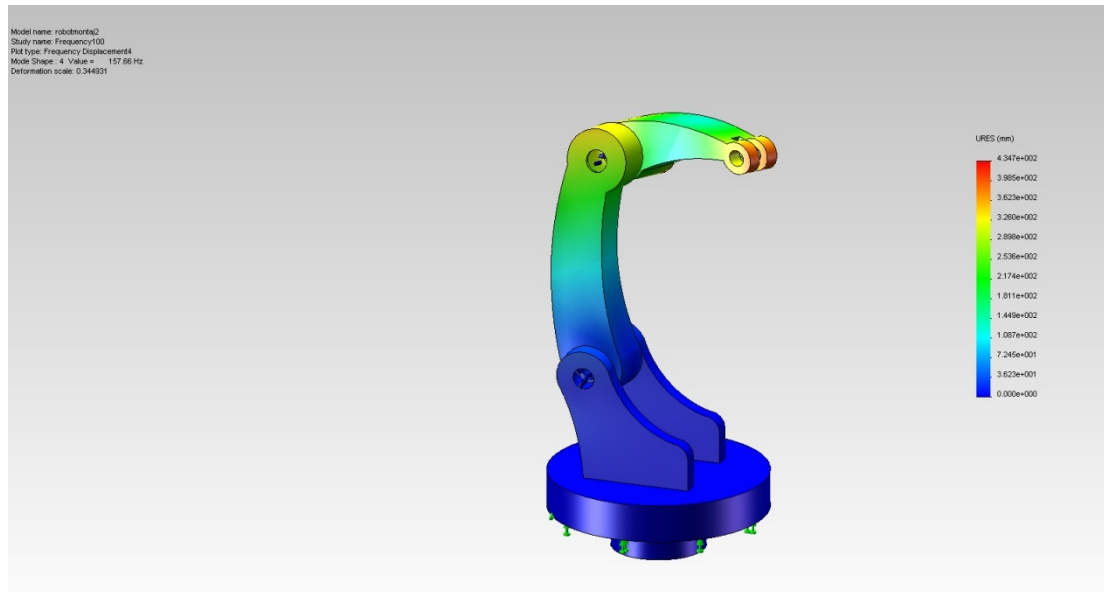


Figure 4.28 The joint angle of the big arm  $\phi_1$  is  $90^\circ$  and the small arm  $\phi_2$  is  $0^\circ$

In this position the natural frequency is 157.66 Hz.

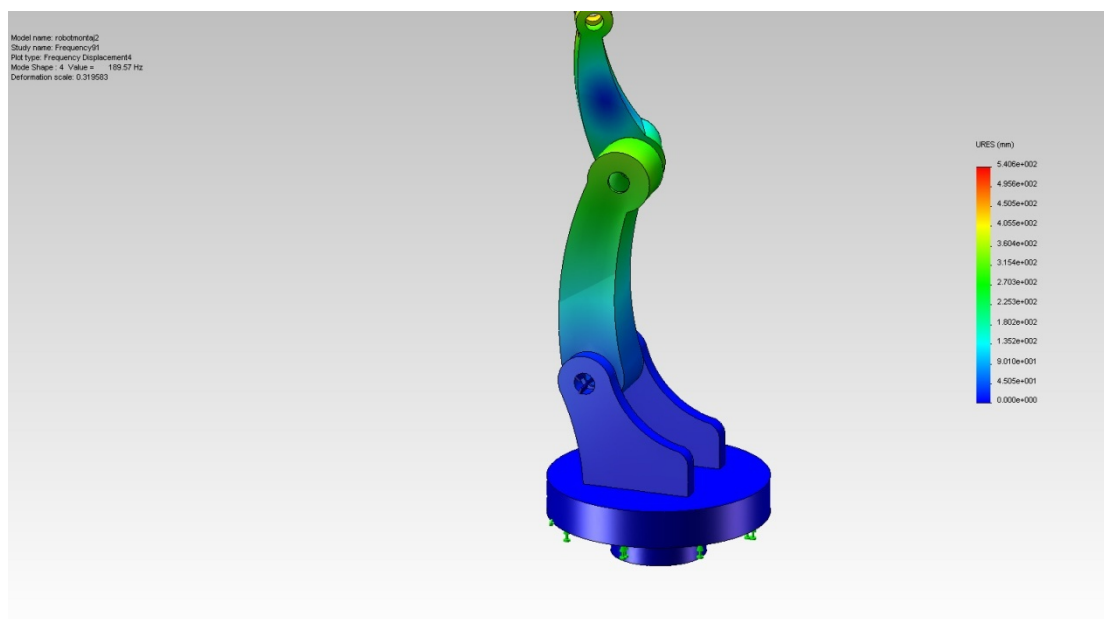


Figure 4.29 The joint angle of the big arm  $\phi_1$  is  $90^\circ$  and the small arm  $\phi_2$  is  $90^\circ$

In this position the natural frequency is 189.57 Hz

In the six frequency spectrum graphics below that made with MATLAB program, we can see clearly the difference in natural frequencies values when we use aluminum material, as shown in Figures 4.30, 4.31, 4.32, 4.33, 4.34 and 4.35.

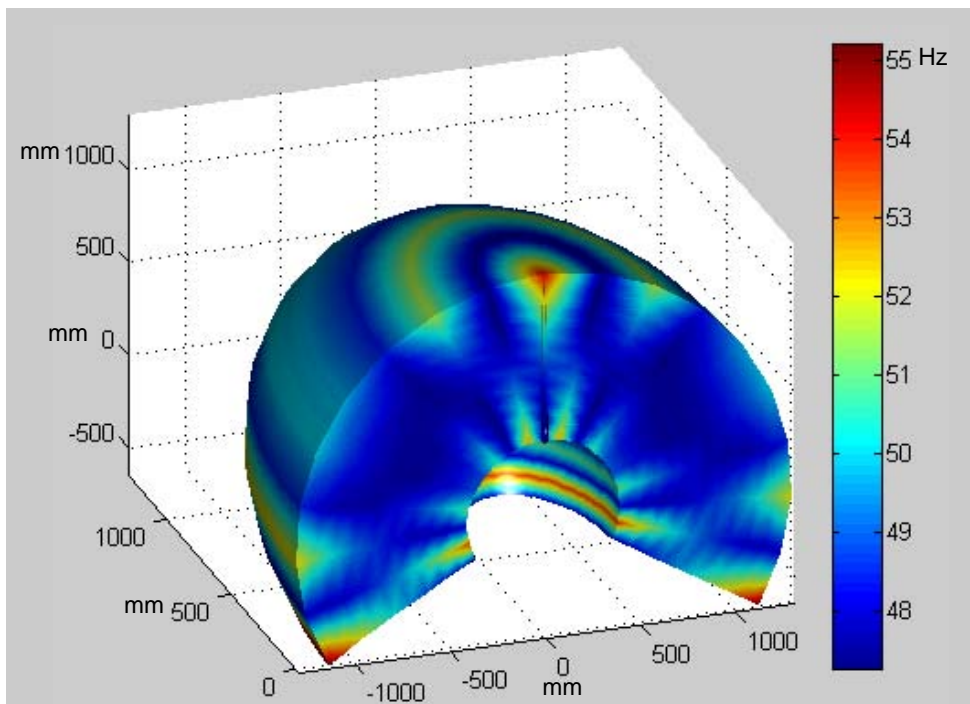


Figure 4.30 The workspace graphic for the first frequency

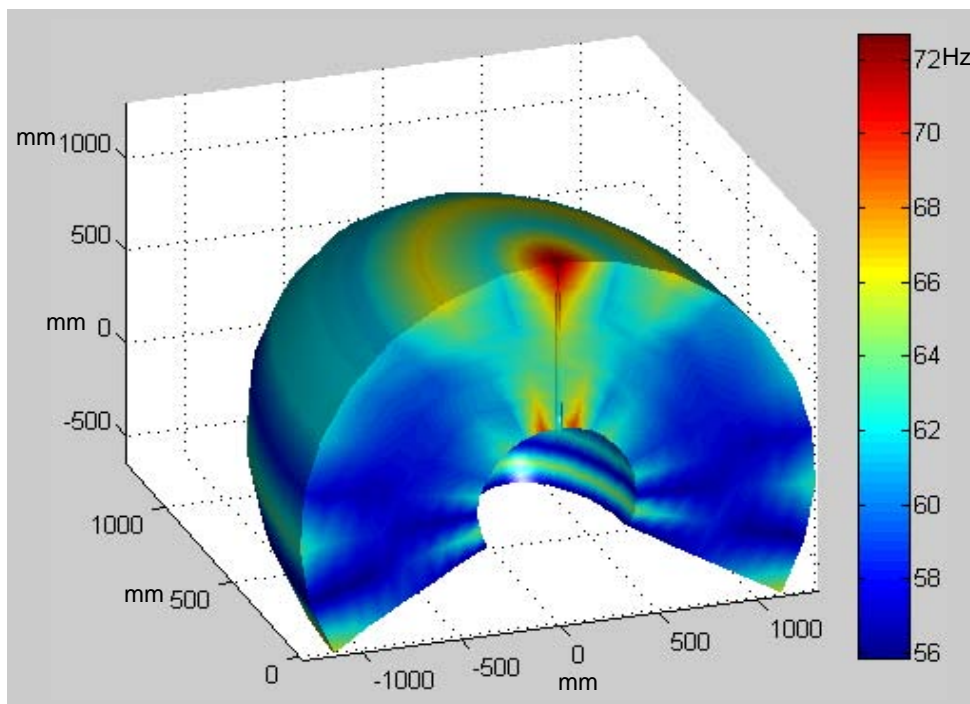


Figure 4.31 The workspace graphic for the second frequency

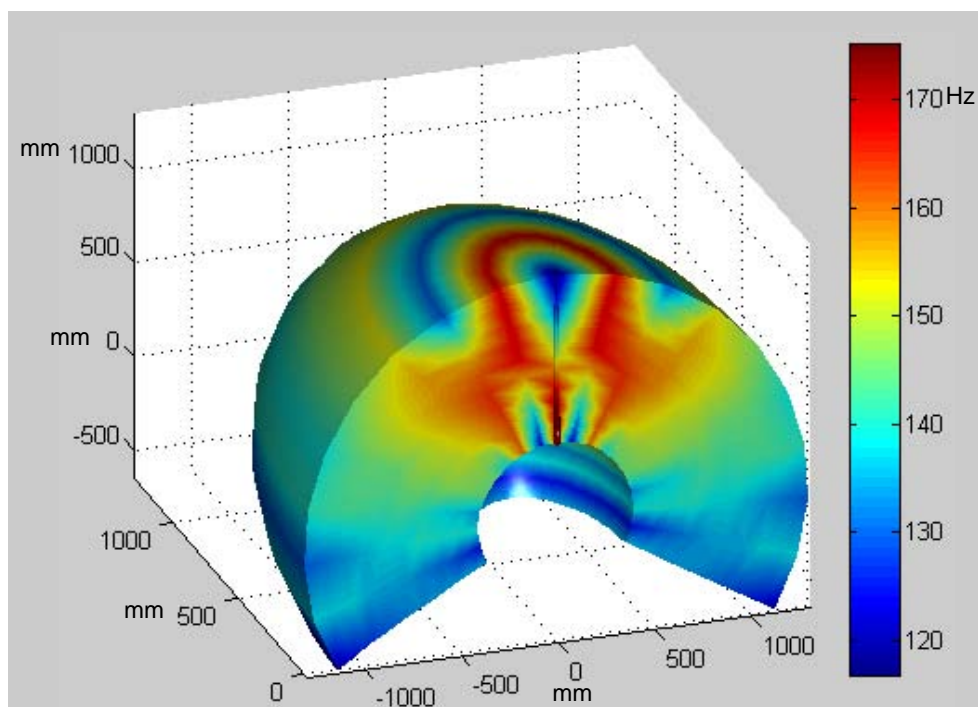


Figure 4.32 The workspace graphic for the third frequency

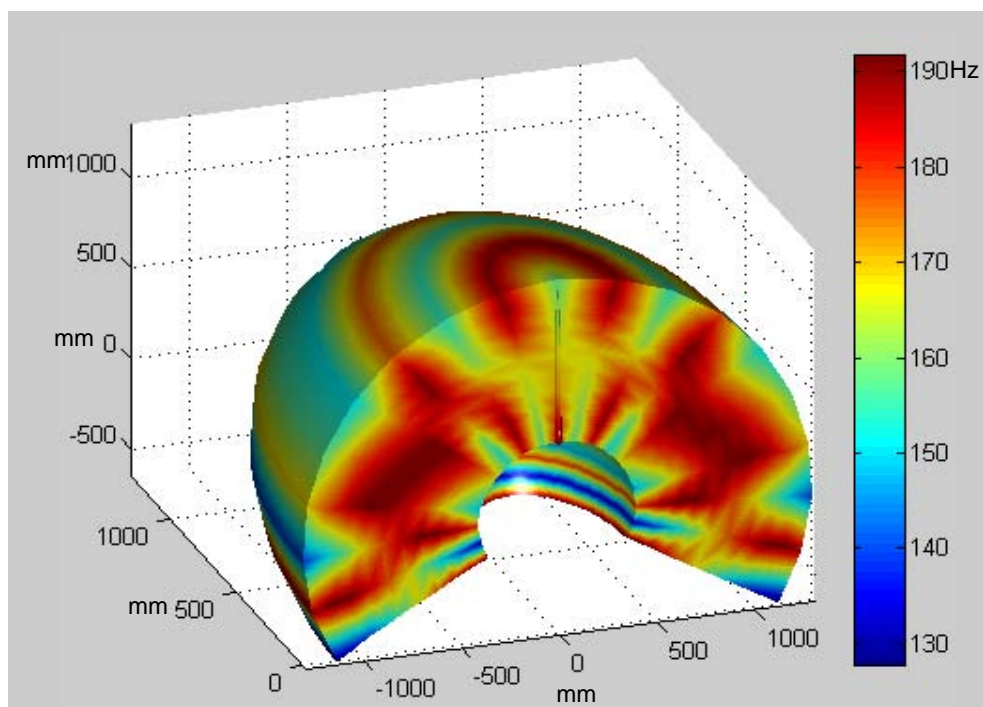


Figure 4.33 The workspace graphic for the fourth frequency

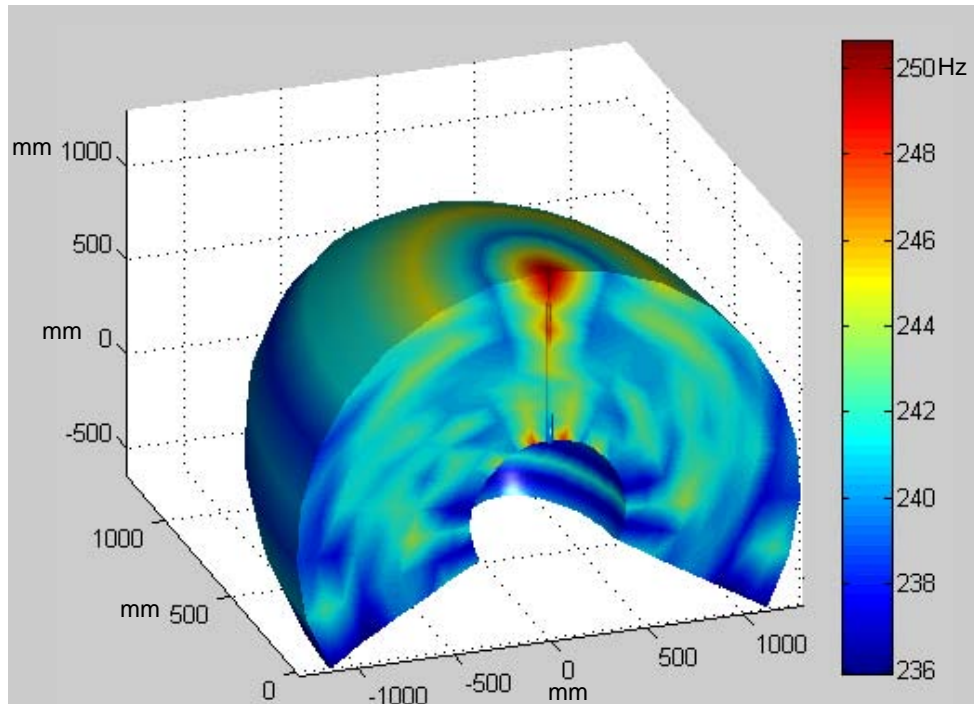


Figure 4.34 The workspace graphic for the fifth frequency

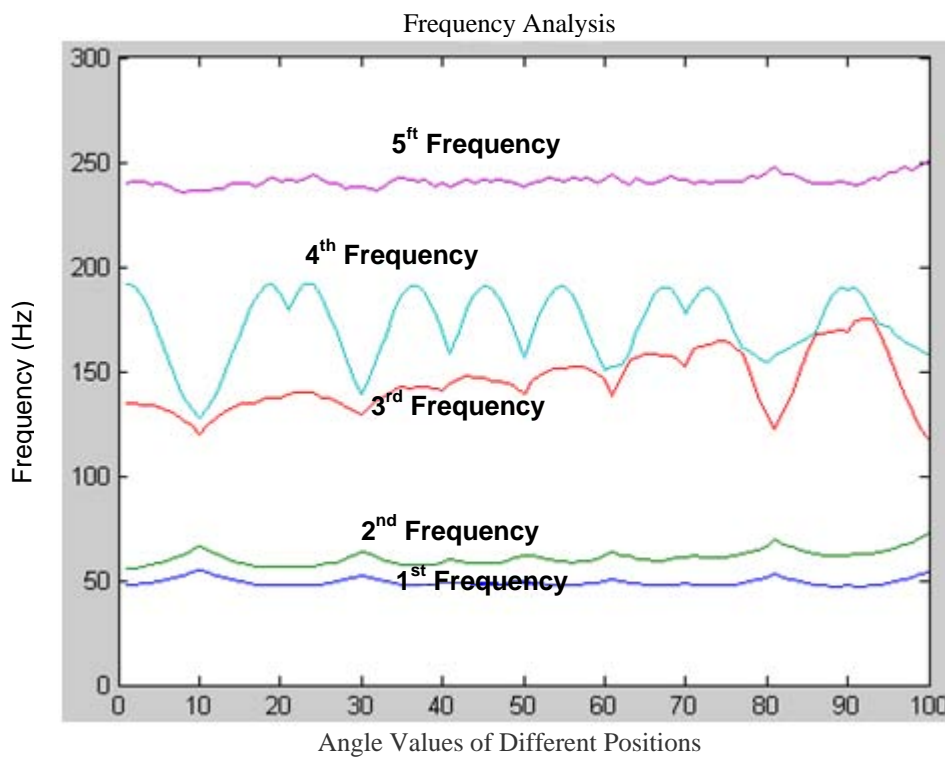


Figure 4.35 The diagram for the five different frequency positions

We can see from the workspace graphics, when we used the pin Connector feature of the Solidworks programme in our analysis, the aluminum material exhibits a few rigidity pattern during the movement of the manipulator.

### 4.3.2 Torsion Spring Coefficient Calculation For The Steel Material:

The equivalent spring coefficient for a torsional spring in the form a cylindrical rod;

$$K_{\theta} = \frac{GxJ_P}{L}$$

$$J = \frac{\pi x D^4}{32}$$

$$G = \frac{E}{2(1 + \nu)}$$

G is shear modulus

J is polar moment of inertia

L : 330 mm = 0,33 m,

D : 70 mm = 0,07 m

$$G = \frac{2 \times 10^{10}}{2(1 + 0,29)} = 7.751937984 \times 10^{10}$$

$$J = \frac{\pi \times 0,07^4}{32} = 2.35598125 \times 10^{-6}$$

$$K_{\theta} = \frac{7.751937984 \times 10^{10} \times 2.35598125 \times 10^{-6}}{0,33} = 553436.9861 \text{ N.m/rad}$$

We used this result in our analysis which we selected to use the pin Connector feature of the Solidworks program. As shown in Figures 4.36 and 4.37 when the big arm angle  $\phi_1$  is  $0^\circ$  and the angular position of the small arm  $\phi_2$  takes value ( $0^\circ$  and  $90^\circ$ ).

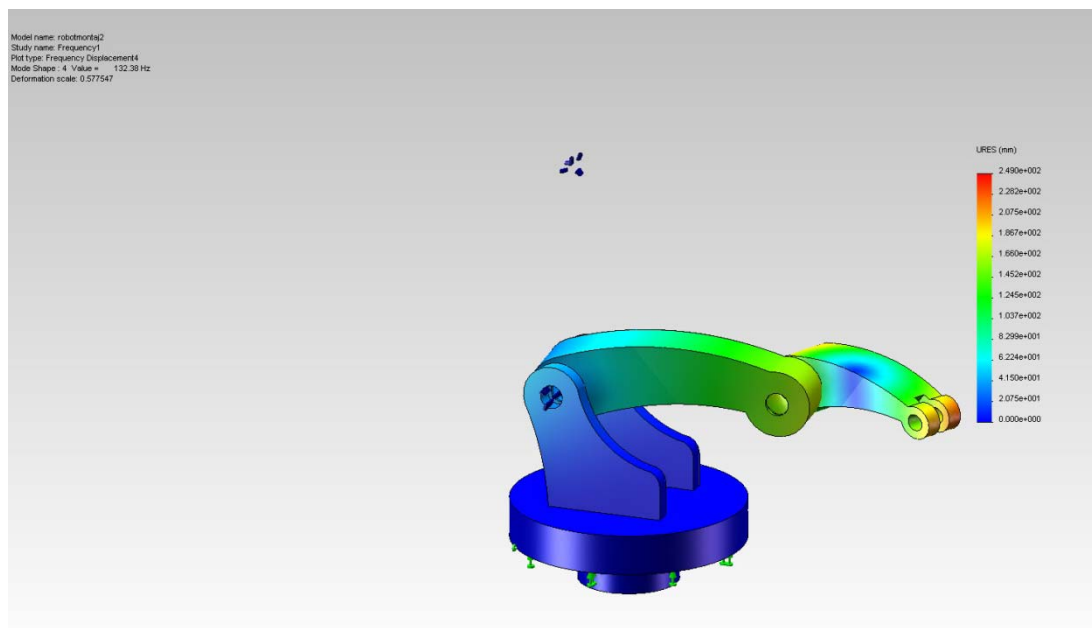


Figure 4.36 The joint angle of the big arm  $\theta_1$  is  $0^\circ$  and the small arm  $\theta_2$  is  $0^\circ$

In this position the natural frequency is 132.30 Hz

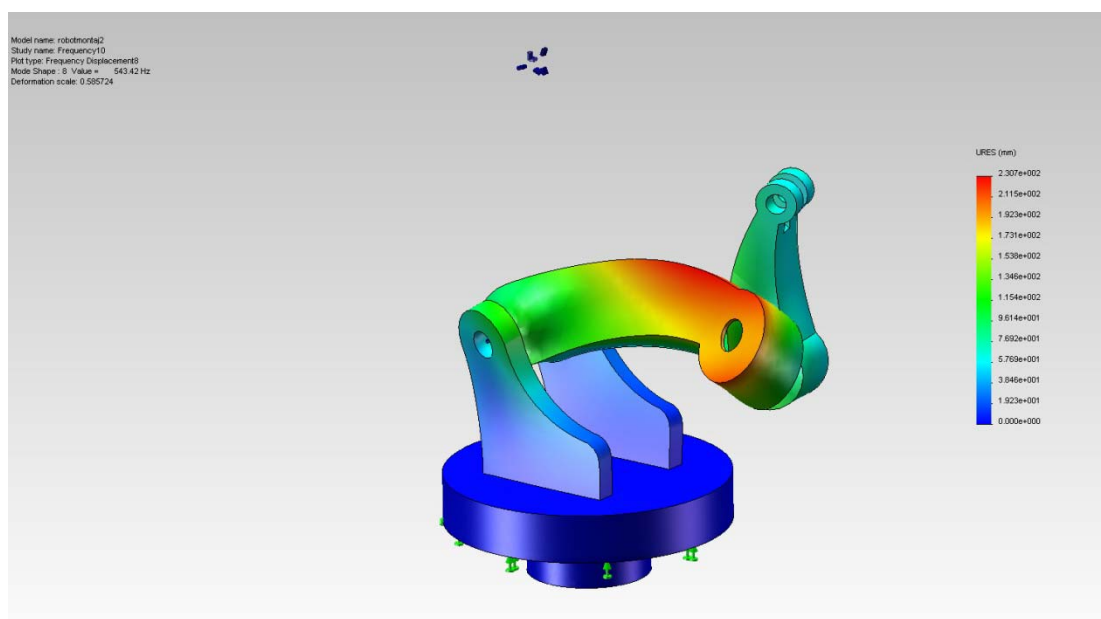


Figure 4.37 The joint angle of the big arm  $\theta_1$  is  $0^\circ$  and the small arm  $\theta_2$  is  $90^\circ$

In this position the natural frequency is 543.42Hz

Finally, in our analyses we selected to use the pin Connector feature of the Solidworks programme. As shown in Figures 4.38 and 4.39 when the big arm angle  $\phi_1$  is  $90^\circ$  and the angular position of the small arm  $\phi_2$  take value ( $0^\circ$  and  $90^\circ$ ).

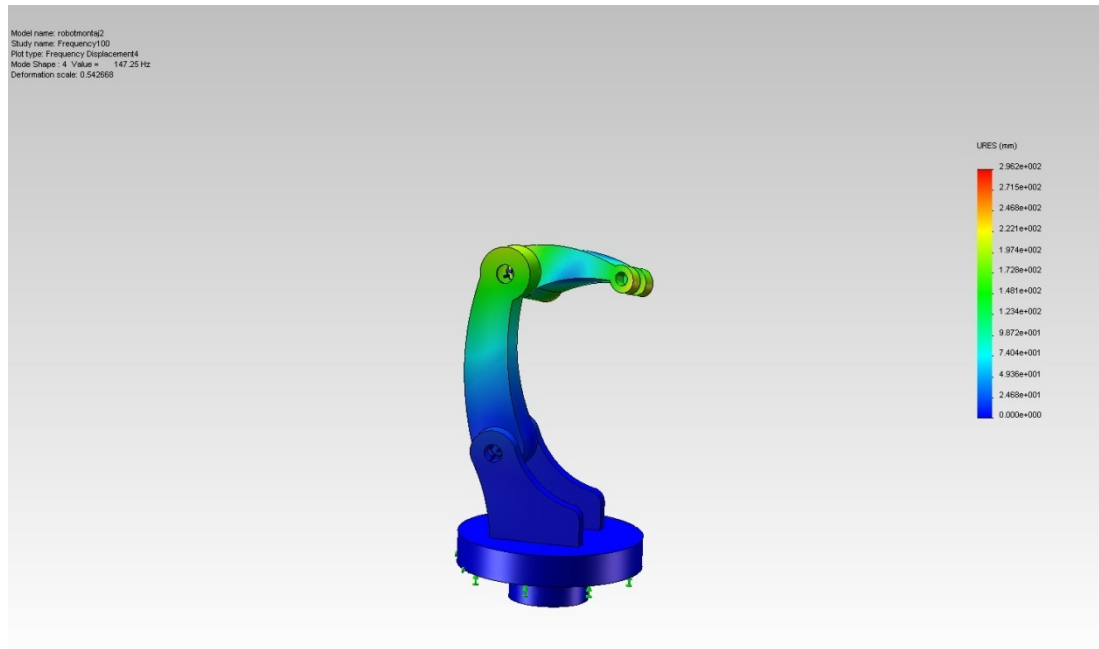


Figure 4.38 The joint angle of the big arm  $\phi_1$  is  $90^\circ$  and the small arm  $\phi_2$  is  $0^\circ$

In this position the natural frequency is 147.25 Hz

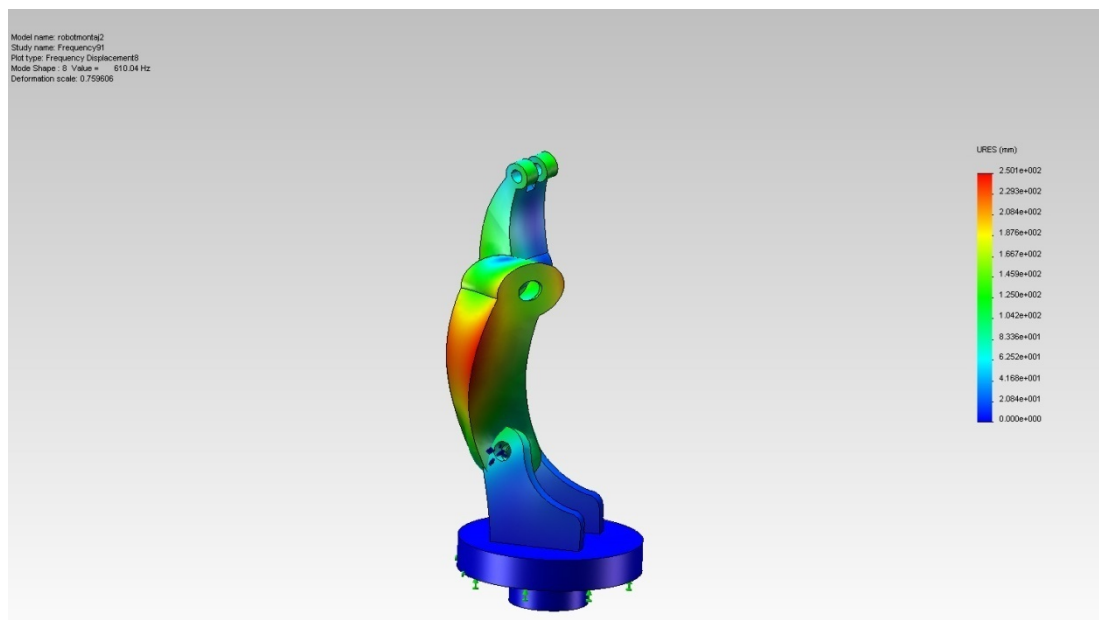


Figure 4.39 The joint angle of the big arm  $\phi_1$  is  $90^\circ$  and the small arm  $\phi_2$  is  $90^\circ$

In this position the natural frequency is 610.04 Hz.

In the six frequency spectrum graphics below which was constructed by MATLAB program, we can see clearly the difference in natural frequencies values when we use steel material. As shown in Figures 4.40, 4.41, 4.42, 4.43, 4.44 and 4.45.

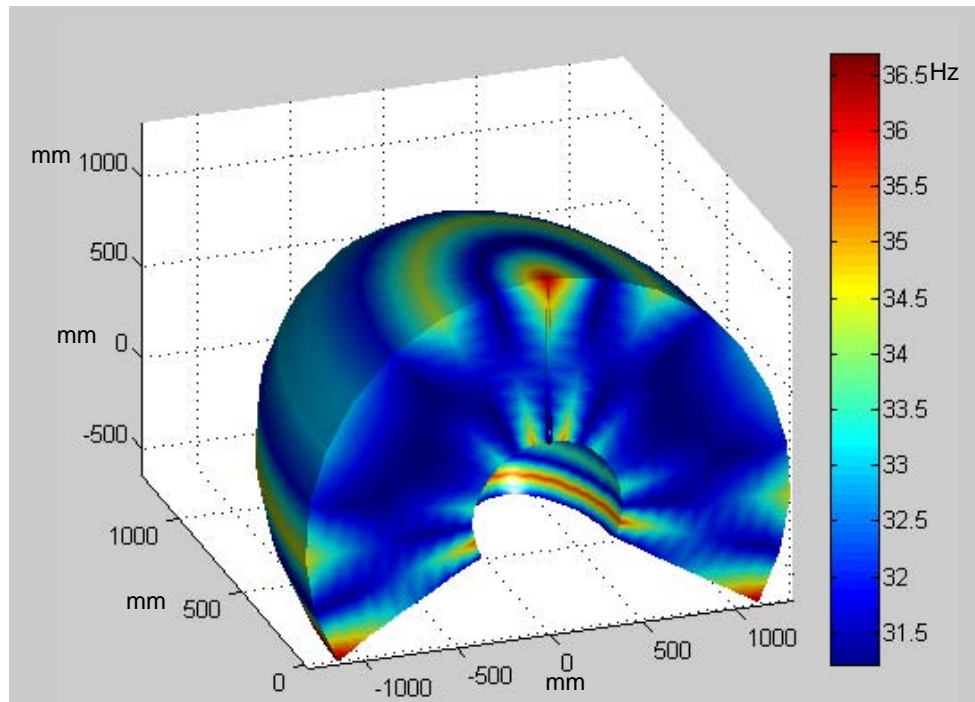


Figure 4.40 The workspace graphic for the first frequency

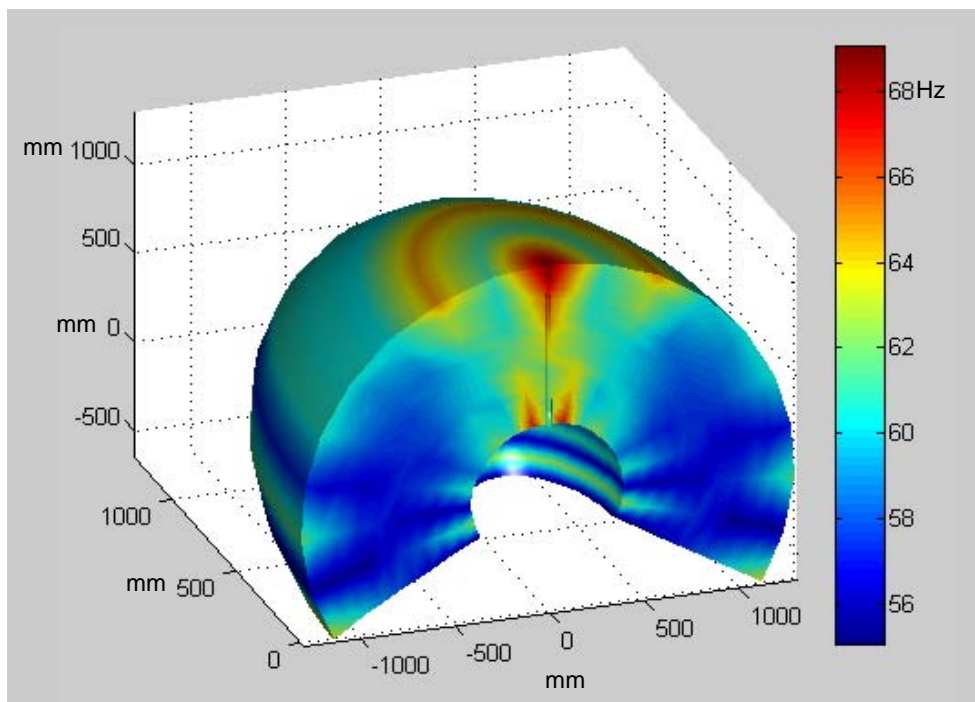


Figure 4.41 The workspace graphic for the second frequency



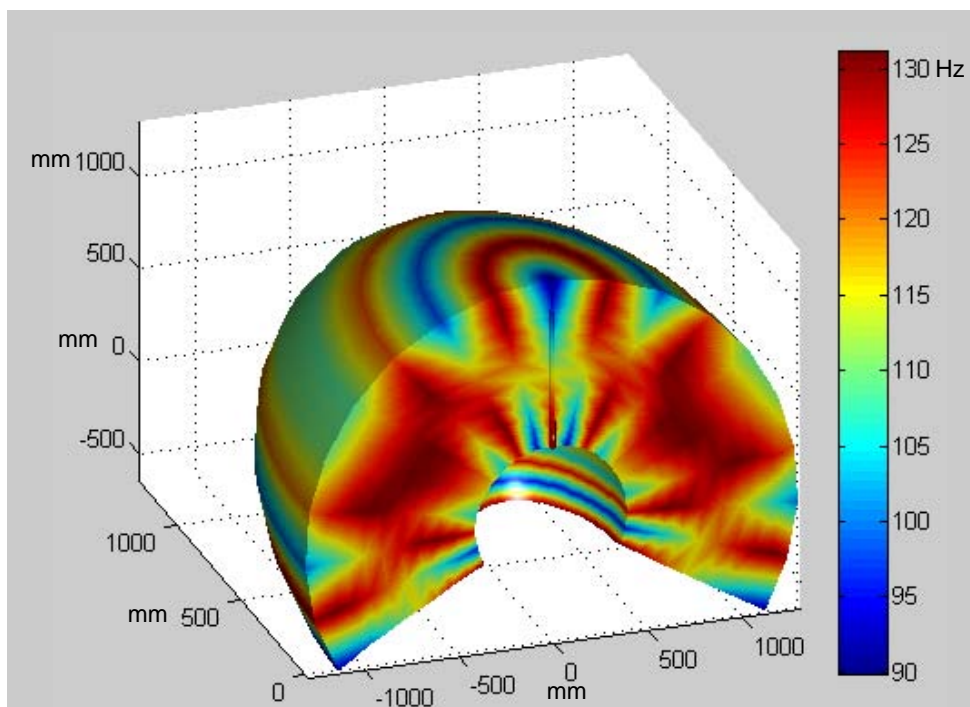


Figure 4.42 The workspace graphic for the third frequency

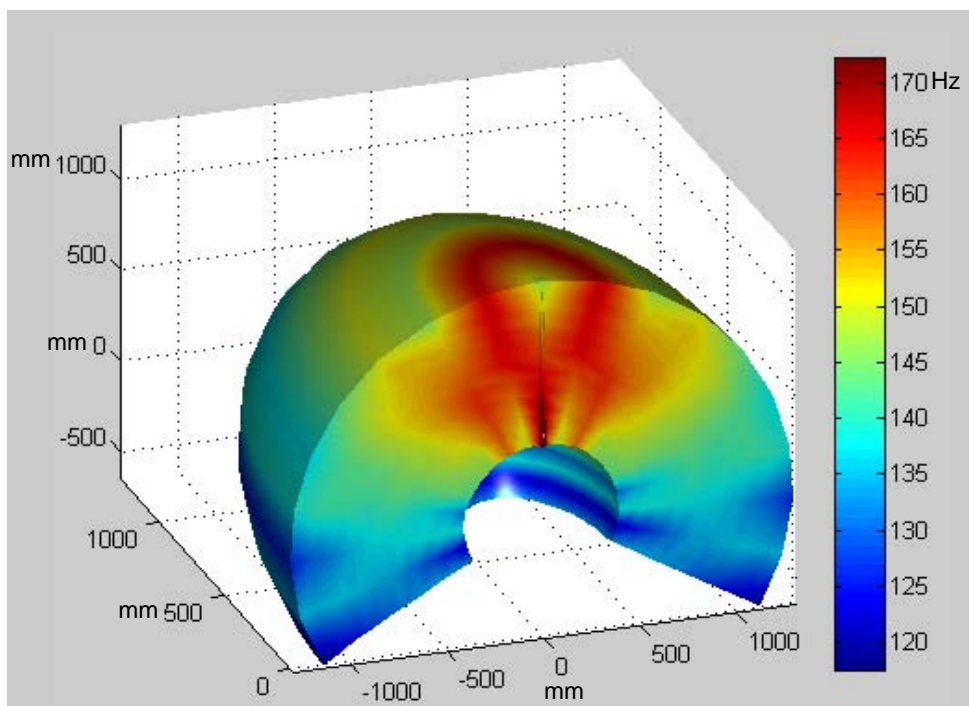


Figure 4.43 The workspace graphic for the fourth frequency

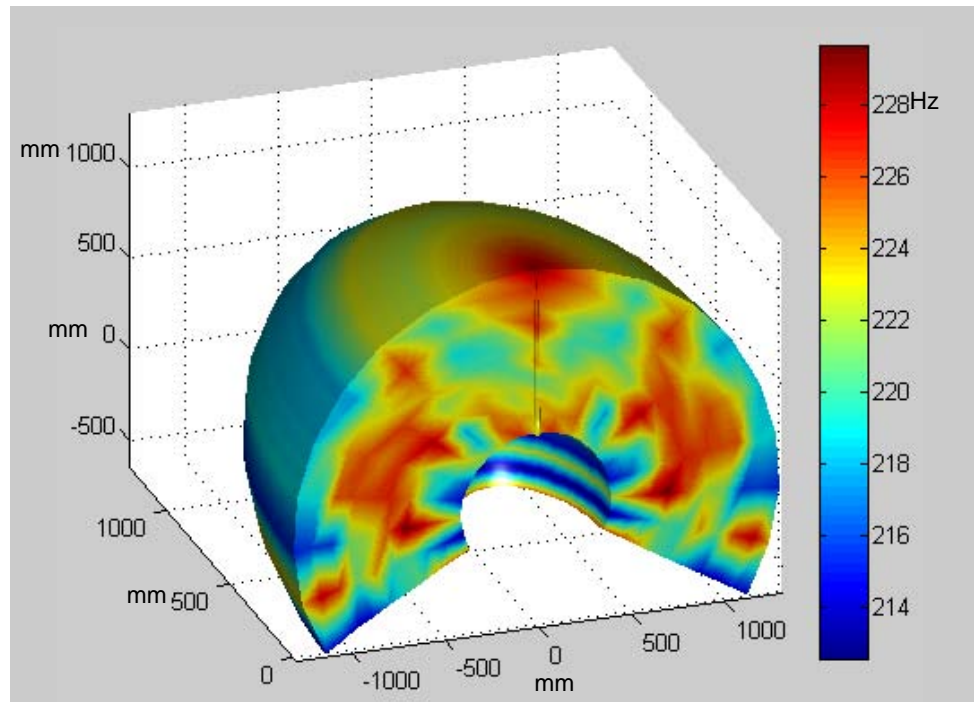


Figure 4.44 The workspace graphic for the fifth frequency

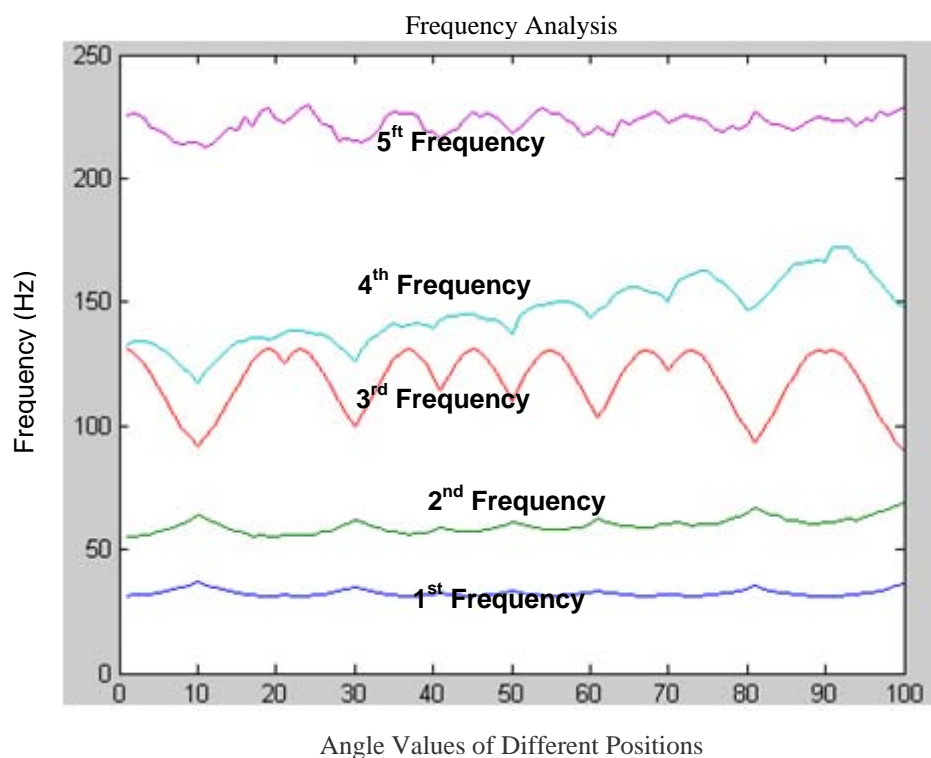


Figure 4.45 The diagram for the five different frequency positions

We can see from the workspace graphics, when we used the pin Connector feature of the Solidworks program in our analysis, steel material exhibits more rigidity pattern during the movement of the manipulator from the aluminum material.

## **CHAPTER FIVE**

### **CONCLUSIONS AND SUGGESTIONS**

Robots have a very significant position among the production tools in today's technology. The robots which execute the transactions such as mounting, painting, transportation, blanking, welding, section feeding, peening, supervision and drilling in the sectors such as automotive, machine production, textile, electronic, chemistry, food and medicine. Robots are preferred in industry and service sectors for the features such as sensitive production, being calculable, acquiring rapid and high quality products, existing in the conditions in which human cannot work and saving from the labor force, although their usage areas are different.

The selection and design of the serial and parallel manipulators are executed in accordance with the basic measures such as load capacity, precise positioning, iteration and rigidity in respect to the usage places and requirements. Computer-aided Engineering tools are utilized for fulfilling the requirements such as selection of the degrees of freedom and making the necessary geometric designation. In consequence of the computer based analyses and designs, the most effective manipulator selection is made and savings in respect of the costs is provided which is one of the most significant problems of the industry.

In this study, natural frequency analyses have been made by using the method of finite elements for the different positions of three independence grade serial manipulators in the study space. Then the finite elements analyses were repeated and the diversion of the natural frequencies were observed by changing the materials of the parts and rigidities of the junction pieces. The primary five natural frequency values for 190 different positions in the study space of the robot have been shown in three dimension graphics with the programme which was developed in MATLAB programme.

The analyses have been made by using steel and aluminum materials and it has been observed that the steel material exhibits a more rigid pattern during the movement of the manipulator. Then, the equivalent arc parameters were calculated in accordance with the material features and geometry of these junction pieces by removing the junction pieces. The effect of the equivalent arc parameters to the flexibility of the system was examined by utilizing from the pin connector feature of the SolidWORKS programme. The acquired results were shown in three dimensional graphics in study space.

Although the analyses results indicates that the manipulator which was derived from steel material is more rigid in the study space, we cannot reach the conclusion that steel material is effective for each usage area. Whether the flexibility of the system remains in acceptable limits for each of two materials, there can be areas in which aluminum material is preferred for reducing the weight and cost. Besides in consequence of the numeric analyses, it has been observed that juncture flexibility changes have significant effect on the natural frequencies of the robot manipulators.

The numeric analyses in this study, were made for a serial manipulator for experiment purposes and its experiments on a robot on production were not executed. In the following phase, the production of the serial manipulator for experiment purposes and its experiments has been fulfilled and the natural frequency results which were gained computer based software can be compared with the experiment results. Besides, orbit control can be made by adding a wrist to provide the orientation into the edge part of the manipulator and the sensitive positioning of the edge point can be provided. Thus, the production of the serial manipulator for experiment purposes can be provided as per the needs of the industry.

## REFERENCES

- Abderrahim, M. and Whittaker, A.R. (2000). Kinematic model identification of industrial manipulators. *Robotics and Computer Integrated Manufacturing*, 16,1-8.
- Akdağ M. (2008). Design and Analysis of Robot Manipulators by Integrated CAE Procedures. 10 Haziran 2009, [http://www.fbe.deu.edu.tr/ALL\\_FILES/Tez\\_Arsivi/2008/DR\\_t544 .pdf](http://www.fbe.deu.edu.tr/ALL_FILES/Tez_Arsivi/2008/DR_t544.pdf)
- Akdağ M. and Kiral Z. (2007). Dynamic Stress Analysis of a Robot Manipulator for Different End Point Trajectories. *Ifac Workshop Technology Transfer in Developing Countries: Automation in Infrastructure Creation – TT*
- Albu-Schaffer, A., Haddadin, S., Ott, C., Stemmer, A., Wimböck, T. and Hirzinger, G. (2007). The DLR lightweight robot: design and control concepts for robots in human environments. *Industrial Robot*, 34 (5), 376-385.
- Alici, G., and Shirinzadeh, B. (2005). A systematic technique to estimate positioning errors for robot accuracy improvement using laser interferometry based sensing. *Mechanism and Machine Theory*, 40, 879-906.
- Bergan, P.B. Horrigmoe, G., Krakeland, B. and Soreide, T.H. (1978). Solution techniques for non-linear finite element problems. *International Journal for Numerical Methods in Engineering*, 12, 1677-1696.
- Bhatia, P. Thirunarayanan, J. and Dave, N. (1998). An expert system-based design of SCARA robot. *Expert Systems with Applications* 15, 99-109.
- Chin, J.-H. and Lin, S-T. (1997). The path precompensation method for flexible arm robot. *Robotics and Computer Integrated Manufacturing*, 13 (3), 203-215.
- Clark, S. and Lin, Y.J. (2007). CAD tools integration for robot kinematics design assurance with case studies on PUMA robots. *Industrial Robot*, 34 (3), 240-248.
- Cleghorn, W. L., Fenton, R. G. and Tabarrok, B. (1981). *Mechanism and Machine Theory*, 16(4), 407-424.

- Craig, J.J. (1986). *Introduction to robotics mechanics & control*. (1th ed.). United States of America: Addison-Wesley.
- Drouet, P., Dubowsky, S. and Mavroidis, C. (1998). Compensation of Geometric and elastic deflection errors in large manipulators based on experimental measurements: application to a high accuracy medical manipulator. 6<sup>th</sup> *International Symposium on Advances in Robot Kinematics*, Austria.
- Dwivedy, S.K. and Eberhard, P. (2006). Dynamic analysis of flexible manipulators, a literature review. *Mechanism and Machine Theory*, 41, 749-777.
- Gaultier, P. E. and Cleghorn, W. L. (1989). *1st National Applied Mechanics Conference*, Cincinnati, OH, pp. 1-10.
- Gaultier, P. E. and Cleghorn, W. L., (1992). *Mechanism and Machine Theory*, 27(4), 415-33.
- Gogate, S. and Lin, Yueh-Jaw, (1992). *Robotica*, 11, 273-282.
- Hibbitt, H.D. and Karlsson, B.I. (1979). Analysis of pipe whip. *EPRI, Report NP*, 1208.
- Jang, J.H., Kim, S.H. Kwak, Y.K. (2001). Calibration of geometric and nongeometric errors of an industrial robot. *Robotica*, 19, 311-321.
- Kalra Parveen and M. Sharan Anand (1991). *Mechanism and Machine Theory*, 26(3), 299-313.
- Karagülle, H. and Malgaca, L. (2004). Analysis of end point vibrations of a two-link manipulator by integrated CAD/CAE procedures. *Finite Elements in Analysis and Design*, 40, 2049-2061.
- Lowen G. G. and Chasspis, C. (1986). *Mechanism and Machine Theory*, 21(1), 33-42.
- Makina Mühendisliği El Kitabı Üretim ve Tasarım. (1995). Cilt 1 TMMOM Makina Mühendisleri Odası Yayın No:170.

Readman, M. C. and Belanger, P. R. (1992). *The International Journal of Robotics Research*, 11(2), 123-134.

Smaili, A. A. (1993). *Mechanism and Machine Theory*, 28(2), 193-205.

Spong, M. W. (1987). *ASME Journal of Dynamic Systems, Measurement and Control*, 109, 310-319.

Yang, Z. and Sadler, J. P. (1990). *ASME Design Technology, Conference*, Chicago IL, 489-496.